NEURAL REGENERATION RESEARCH
www.nrronline.org

Review

Biomaterial and tissue-engineering strategies for the treatment of brain neurodegeneration

https://doi.org/10.4103/1673-5374.336132

Date of submission: August 16, 2021

Date of decision: September 30, 2021

Date of acceptance: October 29, 2021

Date of web publication: February 28, 2022

From the Contents

Bridget Martinez[1, #], Philip V. Peplow[2, *, #]

Abstract

The incidence of neurodegenerative diseases is increasing due to changing age demographics and the incidence of sports-related traumatic brain injury is tending to increase over time. Currently approved medicines for neurodegenerative diseases only temporarily reduce the symptoms but cannot cure or delay disease progression. Cell transplantation strategies offer an alternative approach to facilitating central nervous system repair, but efficacy is limited by low *in vivo* survival rates of cells that are injected in suspension. Transplanting cells that are attached to or encapsulated within a suitable biomaterial construct has the advantage of enhancing cell survival *in vivo*. A variety of biomaterials have been used to make constructs in different types that included nanoparticles, nanotubes, microspheres, microscale fibrous scaffolds, as well as scaffolds made of gels and in the form of micro-columns. Among these, Tween 80-methoxy poly(ethylene glycol)-poly(lactic-co-glycolic acid) nanoparticles loaded with rhynchophylline had higher transport across a blood-brain barrier model and decreased cell death in an *in vitro* model of Alzheimer's disease than rhynchophylline or untreated nanoparticles with rhynchophylline. In an *in vitro* model of Parkinson's disease, trans-activating transcriptor bioconjugated with zwitterionic polymer poly(2-methacryoyloxyethyl phosphorylcholine) and protein-based nanoparticles loaded with non-Fe hemin had a similar protective ability as free non-Fe hemin. A positive effect on neuron survival in several *in vivo* models of Parkinson's disease was associated with the use of biomaterial constructs such as trans-activating transcriptor bioconjugated with zwitterionic polymer poly(2-methacryoyloxyethyl phosphorylcholine) and protein-based nanoparticles loaded with non-Fe hemin, carbon nanotubes with olfactory bulb stem cells, poly(lactic-co-glycolic acid) microspheres with attached DI-MIAMI cells, ventral midbrain neurons mixed with short fibers of poly-(L-lactic acid) scaffolds and reacted with xyloglucan with/without glial-derived neurotrophic factor, ventral midbrain neurons mixed with Fmoc-DIKVAV hydrogel with/without glial-derived neurotrophic factor. Further studies with *in vivo* models of Alzheimer's disease and Parkinson's disease are warranted especially using transplantation of cells in agarose micro-columns with an inner lumen filled with an appropriate extracellular matrix material.

Key Words: Alzheimer's disease; biomaterial; cell transplantation; neurodegeneration; neurodegenerative disease; Parkinson's disease; tissue-engineering; traumatic brain injury

Introduction

Aging is the main risk factor for neurodegeneration, with 30 million people estimated to be affected by neurodegenerative diseases worldwide (Vanni et al., 2020). It is difficult to understand the mechanism underlying the onset and propagation in these diseases due to different region-specific presentations and cell-cell communication, and which hampers the development of effective treatments. Regarding brain injury, there are more than 80 million people who have experienced a stroke (Lindsay et al., 2019) and 69 million individuals worldwide are estimated to sustain a traumatic brain injury each year, many being sports-related injuries (Theadom et al., 2020) or from road traffic accidents (Dewan et al., 2018).

The loss of functional neurons in the central nervous system (CNS) in neurodegenerative diseases and brain injuries causes substantial deterioration in the quality of life. They place a very high burden on families and health care systems (Peplow et al., 2021). A lack of innate cellular repair mechanisms in the CNS inhibits the restoration of the damaged brain. Moreover, a loss of axonal pathways frequently occurs in neurodegenerative diseases and brain injuries (Levin et al., 1983; Marshall et al., 1988; Cheng et al., 2010; Tallantyre et al., 2010), and natural regeneration of these long axon pathways is impaired by endogenous inhibition of axon growth and absence of directed guidance to far distant targets (Levin et al., 1983; Marshall et al., 1988; Curinga and Smith, 2008; Huebner and Strittmatter, 2009; Cheng et al., 2010; Tallantyre et al., 2010). The FDA-approved medicines for neurodegenerative diseases such as Alzheimer's disease and Parkinson's disease only reduce the symptoms for a limited time and do not cure or delay the progression of the disease.

Strategies using cell replacement and promoting axonal outgrowth and guidance are currently being used to facilitate CNS repair. Stem cells obtained endogenously or delivered from exogenous sources are most commonly used in cell replacement strategies (Horner and Gage, 2000; Kim and de Vellis, 2009; Trueman et al., 2013). While some functional recovery has been shown in animal models using cell transplantation therapies, their efficacy has been limited by low *in vivo* survival rates of cells injected in suspension (Anderson et al., 2011; Kriks et al., 2011; Nakaji-Hirabayashi et al., 2013; Cordeiro et al., 2014; Yamauchi et al., 2015). Advantages of stem cell therapies include secretion of neuroprotective factors, providing glia to remyelinate denuded axons, and in some cases providing new neurons to discrete regions (Tate et al., 2002, 2004; Shear et al., 2004; Cummings et al., 2005; Orlacchio et al., 2010; Kim, 2011). While the transplantation of dissociated cells has received great attention to repair the brain, it cannot restore key anatomic features of damaged pathways, most notably long axon tracts. To restore long-distance axonal connections, studies typically aim to create a permissive environment of axonal outgrowth (Stichel et al., 1999; Bradbury et al., 2002; Mingorance et al., 2006; Tang et al., 2007) and/or promote the intrinsic capacity of axons to regenerate (Jain et al., 2004; Liu et al., 2010; Yip et al., 2010). These strategies most commonly involve biomaterial or cellular scaffolds to increase growth-promoting cues, decrease inhibitory factors, and/or augment the regenerative capacity of individual axons (Borisoff et al., 2003; Tsai et al., 2004; Moore et al., 2006; Filous et al., 2010; Silva et al., 2010). An ability to promote and guide axonal regeneration has been shown by these approaches (Tsai et al., 2004; Cai et al., 2005; Moore et al., 2006; Wen and Tresco, 2006a,b; Cullen et al., 2008; Kim et al., 2008; Silva et al., 2010), but do not address degeneration of source neuronal population(s). While the survival of transplanted neural cells and modest axonal outgrowth/guidance have been demonstrated, neuronal replacement together with targeted axonal regeneration to appropriate targets remains a major challenge.

Tissue engineering, using biomimetic scaffolds made of natural or synthetic material and enclosing cells, has the potential to regenerate damaged or lost tissues (Zamproni et al., 2021). The scaffold provides cell support and allows the exchange of oxygen, nutrients, growth factors, and cytokines between cells and medium. Such biomimetic scaffolds attempt to reproduce the

[1]Department of Medicine, St. Georges University School of Medicine, Grenada; [2]Department of Anatomy, University of Otago, Dunedin, New Zealand

***Correspondence to:** Philip V. Peplow, PhD, phil.peplow@otago.ac.nz.

https://orcid.org/0000-0001-5468-1989 (Philip V. Peplow)

#Both authors contributed equally to this article.

How to cite this article: *Martinez B, Peplow PV (2022) Biomaterial and tissue-engineering strategies for the treatment of brain neurodegeneration. Neural Regen Res 17(10):2108-2116.*

conditions of the extracellular matrix (ECM), and need to possess a series of characteristics such as biodegradability and absence of an immune response by the host tissue, suitable mechanical properties, suitable porosity and permeability, and able to be produced on a large scale and in a reproducible way (Owen and Shoichet, 2010). In preparing for conventional transplantation procedure, cells must be first enzymatically detached from a 2D culture surface and dissociated into a single cell suspension, thereby disrupting cell-cell and cell-material interactions and damaging any previously formed neuronal connections. Upon detachment from the ECM and neighboring cells, anchorage-dependent cells undergo apoptosis (Marchionini et al., 2003). Culturing cells within a transplantable 3D biomaterial scaffold has the advantage of a matrix environment that can maintain these cell-cell and cell-material interactions, leaving adherent neuronal networks intact, during the transition to a potentially damaging *in vivo* location. A suitable 3D scaffold is able to mimic the *in vivo* microenvironment more closely than 2D culture substrates (Francis et al., 2016).

Functionalized self-assembling peptides (SAPs) are a new class of biosynthetic materials with potential in the development of scaffolds for 3D cell cultures (Zhang et al., 2005; Zhang, 2008). SAPs have > 90% water content and are of peptide molecules that can break down into natural amino acids, which can potentially be used by the cells. Various SAPs have successfully been used for neural cell culture. An amphiphilic molecule containing the IKVAV (isoleucine-lysine-valine-alanine-valine) motif, an epitope derived from laminin, stimulated the differentiation of several progenitor cells into neurons (Silva et al., 2004). RADA16-like SAPs (the RADA motif refers to arginine, alanine, aspartic acid, alanine) are composed of natural amino acids that spontaneously self-assemble under physiologic conditions into antiparallel β-sheets forming nano- and micro-fibers and closely mimic the ECM architecture. Using pheochromocytoma 12 (PC12) cells, RADA16-I and RADA16-II-induced neurite outgrowth and synapse formation (Holmes et al., 2000). RADA16-I enhanced the proliferation and differentiation of neural stem cells (NSCs) (Gelain et al., 2006), attracted migrating hippocampal neural cells, which are potential neuroprogenitors, at the interface between hippocampal slices and biomaterial (Semino et al., 2004), and promoted neurite outgrowth of a PC12 cell line (Li and Chau, 2010). RADA16-I is a 16-residue peptide composed of alternating hydrophilic arginine (R), hydrophobic alanine (A), and hydrophilic aspartic acid (D) units (RADARADARADARADA) and is the most used SAP for neural cell culture (Wang et al., 2019). RADA16-I can be synthesized commercially with high purity and can be custom-tailored to incorporate functional motifs for specific cell culture applications for neurons or other cell types. The aim of this review was to analyze the research literature describing recent biomaterial and tissue engineering strategies to promote neural repair and function in animal models of neurodegenerative disease and traumatic brain injury.

Biomaterial and Tissue Engineering Strategies to Promote Neuronal Survival and Function

We performed a PubMed search for original research articles published January 2009–April 2021 on the production and use of biomaterial and tissue-engineered constructs to promote neuronal survival and neurite outgrowth in *in vitro* and *in vivo* studies. The steps involved in the review and its contents are shown (**Figure 1**). A total of 15 articles were found for this review and the relevant findings are summarized in the following sections.

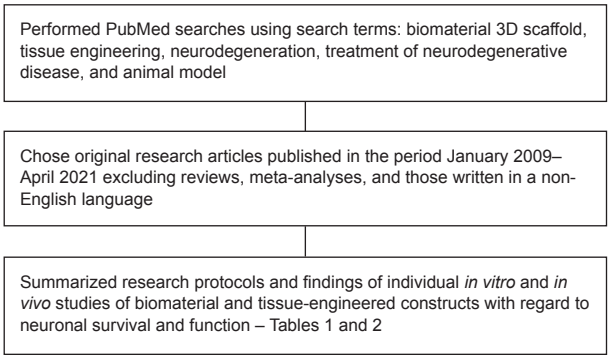

Figure 1 | **Flow diagram to indicate how the review was performed and its contents.**

Nanoparticles delivery and carbon nanotubes for cell engraftment

Xu et al. (2020) prepared rhynchophylline (RIN) loaded methoxy poly(ethylene glycol)-poly(lactic-co-glycolic acid) (mPEG-PLGA) nanoparticles (NPS). RIN is a major active tetracyclic oxindole alkaloid stem from traditional Chinese medicine Uncaria species, and has potential activities in the treatment of Alzheimer's disease and stroke (Fu et al., 2014; Shao et al., 2015). Tween 80 was added to the NPS solution and stirred slowly to facilitate T80-NPS-RIN formation. The mean particle size was 145 nm. T80-NPS-RIN had significantly higher transport across an *in vitro* brain-blood barrier model (endothelial barrier layer) compared to RIN or NPS-RIN, with drug accumulation increasing with time and reaching permeability saturation after 3 hours. In a biodistribution study using C57BL/6 mice divided into three groups (n = 5/group) and injected with 200 μL of DiD, NPS-DiD and T80-NPS-DiD solution via tail vein (DiD, 1,1′-dioctadecyl-3,3,3′,3′- tetramethylindo-dicarbocyanine, 4-chlorobenzenesulfonate salt is a fluorescent dye),

T80-NPS-DiD had significant distribution in the brain compared to free DiD and NPS-DiD. The DiD fluorescence sign in the brain suggested that the T80-NPS had penetrated the brain-blood barrier and was present in the mouse brain. NPS had no brain-targeting effect indicating that the T80 coating is essential for the delivery of drugs into the brain. An apoptosis assay of T80-NPS-RIN to protect mouse pheochromocytoma cells PC12 cells against $A\beta_{25-35}$ injury was performed. PC12 cells (6×10^3/well) were treated with RIN, NPS-RIN, and T80-NPS-RIN (25 μM) for 24 hours. Exposure to 20 μM $A\beta_{25-35}$, which could lead to 50–60% cell death, was used as an Alzheimer's disease model *in vitro*. After 4 hours of 20 μM $A\beta_{25-35}$, the T80-NPS-RIN group at different concentrations markedly decreased the cell death caused by $A\beta_{25-35}$ compared with the RIN group. Upon increasing the concentration of T80-NPS-RIN, a strong protective effect on PC12 cells was seen.

Zwitterionic polymer poly(2-methacryoyloxyethyl phosphorylcholine capsuled protein-based nanoparticles (nBSA) were prepared by Wang et al. (2017). Non-Fe hemin (NFH)-loaded nanoparticles were made by loading the drug onto the nBSA (NFH-nBSA). HIV-1 trans-activating transcriptor (TAT) is a cell-penetrating peptide that was bioconjugated with zwitterionic and protein-based nanoparticles and served as a carrier to increase brain-blood barrier permeability. The sizes of the TAT-modified nanoparticles were ~24 nm. NFH is a natural prototype iron chelator, and obtained by removing the iron core of hemin. An important factor involved in the loss of dopaminergic neurons in Parkinson's disease is oxidative stress, and iron chelation therapy is an effective modality (Lei et al., 2012; Stankowski et al., 2012; Ayton et al., 2013; Weinreb et al., 2013). The *in vitro* anti-Parkinson effect of NFH-loaded nanoparticles was examined using SH-SY5Y cells (human neuroblastoma cell line). The cells were seeded at 1.0×10^4 cells/well in 200 μL medium and incubated for 24 hours when they reach 70–80% confluence. The cells were treated with 100 μL MPTP (1-methyl-4-phenyl-1,2,3,6-tetrahydropyridine, 300 μM) per well for 1 hour. Then serial dilutions of free NFH, NFH-nBSA, and TAT-NFH-nBSA nanoparticles were added into each well. The cells were incubated for 48 hours before MTT assay. Similar cell viability as free NFH was shown by TAT-NFH-nBSA nanoparticles against PD cells in each concentration of NFH. The NFH-nBSA group had little additional anti-Parkinson efficacy as the concentration increased. The reactive oxygen species (ROS) level of PD cells induced by MPTP for 24 hours was determined. NFH-nBSA treated cells did not show any significant decrease in ROS compared to untreated PD cells. TAT-NFH-nBSA nanoparticles caused a marked decrease in ROS compared to untreated PD cells. The *in vivo* anti-Parkinson activities were investigated using MPTP-treated C57BL/6 male mice, 10–11 weeks of age. The mice were divided into six groups (n = 5/group). After a 5-day continuous intraperitoneal injection of MPTP (15 mg/kg), the mice began to show Parkinson's symptoms and a decrease of body weight, and treatment was then started. The mice in the different groups were injected via the tail vein with PBS, NFH-nBSA, and TAT-NFH-nBSA nanoparticles at an NFH dose of 1.2 mg/kg once every 3 days. Compared with the Parkinson group, the groups treated with TAT-NFH-nBSA nanoparticles had a greater increase in body weight. In the NFH-nBSA treated group, the body weight increased slowly especially during the last 10 days. The Parkinsonian symptoms were decreased by treatment with the three different TAT-NFH-nBSA nanoparticles and approached the results of the healthy group, with there being a greater increase in body weight and improvement in two behavioral tests. TAT-5-NFH-nBSA nanoparticles brought about significant behavioral improvement in Parkinsonian mice and were better than TAT-1-NFH-nBSA and TAT-10-NFH-nBSA nanoparticles. By qRT-PCR, the TAT-5-NFH-nBSA group exhibited an increased mRNA level of tyrosine hydroxylase (TH) and dopamine transporter protein in the substantia nigra pars compacta (SNpc) compared to other groups. TH is the rate-limiting enzyme of dopamine biosynthesis in the brain and also a marker for dopaminergic neurons. The amount of dopamine transporter can indirectly reflect the function of dopaminergic neurons in the SNpc and thus dopamine transporter is considered a marker of dopaminergic neurons (Ikea et al., 2019). *In vivo* toxicity evaluation of these four different drug delivery systems was performed on the Parkinsonian mice after treatment for 30 days. The delivery systems were injected via the tail vein once every 3 days for 24 days. No histopathological abnormalities or lesions in the heart, liver, spleen, lung, and kidney were caused by the injected nanoparticles.

Maraei et al. (2017) genetically engineered human olfactory bulb neural stem cells (OBNSCs) to overexpress green fluorescent protein (GFP). Upon reaching 80% confluence, the formed OBNSCs neurospheres were collected and dissociated into single cells by accutase treatment. Multiwalled carbon nanotubes (MWCNT) OD ~50–60 nm, length ~10–20 μm were dissolved in PBS at a concentration up to 100 μg/mL. Neurodegeneration was induced in male Wistar rats, 220 ± 25 g, by intraperitoneal injection of trimethyltin chloride in saline at a dose of 6 mg/kg. At 4 weeks following trimethyltin chloride administration, the lesioned rats were anesthetized and stereotactically injected at CA1 region of the hippocampus with 4 μL of CNT/OBNSCs mixture (1 μL multiwalled carbon nanotubes + 3 μL OBNSCs 15×10^4 cells). For animals receiving grafts, immunosuppression via daily subcutaneous injections of cyclosporine (10 mg/kg) was begun 1 day before grafting and finished on the day of euthanasia. The brain was dissected, and the hippocampus was fixed in 4% paraformaldehyde. The GFP-OBNSCs/CNTs survived in the lesion environment for > 8 weeks after implantation and no tumor formation was observed during 8 weeks. By 8 weeks post engraftment, GFP^+ cells with morphological characteristics suggestive of mature neurons

were recognized. During the 8-week time window, 60%, 17%, and 23% of the engrafted cells were differentiated into neurons, oligodendrocytes, and astrocytes, respectively. At 4 weeks post engraftment of GFP-OBNSCs/CNTs, the CA1 neurons and oligodendrocytes had increased in number with the remnant of necrotic cells. By 8 weeks, restoration of the normal structure had occurred, including pyramidal cell layer thickness.

Microspheres and microscale scaffolds

In a study by Skop et al. (2019) chitosan microspheres were formed by extruding a 3% acid chitosan solution through a syringe with a 30-g needle into a basic coagulation bath, consisting of 2.5 M NaOH:methanol:water (20:30:50 v/v). To create smaller spheres, the electrospray method was used. Heparin was crosslinked to the chitosan microspheres. A traumatic brain injury model was produced by subjecting male Sprague Dawley rats, 2 months of age, to a controlled cortical impact procedure. Neural progenitors (NPs) from the ventricular zone (VZ) of embryonic day 13.5 enhanced GFP rat neocortex were attached to the microspheres with ~3×10^4 VZ NPs attached to ~500 microspheres (each ~50 µm in diameter) and injected directly into the lesion cavity at 7 days following controlled cortical impact. The VZ NPs expressing GFP could be readily distinguished from the host cells using fluorescence microscopy. Most VZ NPs were located in the tissue surrounding the microspheres although some remained adhered to the beads at 3 days after transplantation. These cells (on and around the microspheres) were positive for the stem cell or progenitor markers Nestin and BLBP. Many GFP^+ cells were also positive for the proliferative marker Ki67. At 2 weeks after transplantation, significant wound repair for those rats that had received microspheres with cells was seen at both the gross level and the microscopic level. Microspheres were present within the lesion cavity adjacent to the host tissue but there appeared to be fewer spheres than seen at 3 days. GFP^+ VZ NPs had dispersed into the tissue and away from the microspheres compared with the 3-day time point. Many of the cells spanned several layers of the neocortex, and the lesion cavity was smaller in recipients that had received the VZ NPs on microspheres versus controls that had received cells only or microspheres only. GFP^+ cells at this time point showed features of differentiation toward mature neural cell types. Behavioral studies of rats showed improved recovery on the beam walking task using the VZ NPs on the microspheres versus cells alone, but the behavioral recovery was not evident at 28 days post-transplantation. At 3 days post-transplantation, cells were seen surrounding the microspheres that did not express markers of neural cells. It was shown that they were neutrophils based on positive staining for Ly-6G and negative staining for Iba-1. By 2 weeks posttransplantation, there were fewer Ly-$6G^+$ cells. Increased phagocytosis of GFP^+ VZ NPs or increased immunogenicity was not observed at either time point as determined by Iba-1 staining for macrophages.

Carlson et al. (2015) constructed fibrous substrates by electrospinning poly(desaminotyrosyl tyrosine ethyl ester carbonate) with an average fiber diameter of 3.23 ± 0.06 µm. Accelerated production of human neuronal cells from induced pluripotent stem (iPS) cells, called induced neuronal (iN) cells, was achieved using sets or single transcription factors (Pang et al., 2011; Zhang et al., 2013). To enable injection *in vivo*, 100 µm square "microscale scaffolds" that could be injected through a 21-G needle were created by downscaling the fiber microspun substrates with a vibratome. Human iN cells were seeded in suspension onto microscale scaffolds. Cells in microscale scaffolds matured into βIII-tubulin and MAP-expressing neuronal cells. The average number of live human iN cells in each scaffold was 83 ± 13 (n = 19). Human iN cell survival was assessed after transplantation of scaffold-supported or dissociated cells into the mouse striatum *in vivo*. Male NOD-SCID IL2 Rγc null mice, 20–35 g, were anesthetized and injected with a total volume of 10 µL containing either 1×10^3, 1×10^5 dissociated GFP^+ iN cells, or ~10 scaffolds seeded with GFP^+ iN cells (~85 cells per scaffold) at 6 days after initiating neuronal conversion, resuspended in ice-cold MEM. Cells or cells on scaffolds were injected stereotactically into the striatum. Mice were euthanized 3 weeks after transplantation for quantification of human iN cells within the graft. At 3 weeks after transplantation, immunocytochemistry of a 1.8 mm × 1.8 mm field including the injection site revealed an average survival rate of 5.74 ± 3.16% based on injected scaffold-seeded iN cells, a 38-fold improvement compared with an average survival of 0.15 ± 0.15% of 1×10^5 injected dissociated iN cells. The scaffold-seeded iN cells maintained neurite length (35 ± 8 µm) which was comparable to that of viable, dissociated iN cells (39 ± 15 µm). No difference in inflammatory response was detected between injection modes, and some ingrowth of host tissue into scaffolds was observed. Surviving transplanted iNs expressed neuronal cell adhesion molecule CD56, β-tubulin III, and synaptophysin. Postsynaptic density protein 95 (PSD95) was detected adjacent or colocalized to transplanted GFP-labeled and synaptophysin-expressing iN neurite terminals, suggestive of synaptic integration with host tissue. In all *in vivo* experiments, some human iNs migrated off scaffolds, and minimal scaffold degradation occurred in the 1–3 weeks posttransplantation period.

Pharmacologically active microcarriers (PAMs) were developed by Delcroix et al. (2011) which were biodegradable and non-cytotoxic polymeric microspheres made of poly(lactic-co-glycolic acid) (PLGA), that with a functionalized surface provided an adequate 3D support for the culture of cells and/or for their administration. The PLGA microspheres had an average diameter of 60 µm. PAMs were coated with laminin and poly-D-lysine, and designed to release neurotrophin 3 (NT3), which stimulate the neuronal-like differentiation of MIAMI cells (marrow-isolated adult multilineage inducible cells) and promote neuronal survival. Whole bone marrow was obtained from vertebral bodies (T1-L5) of a 3-year-old male cadaveric donor. Whole bone marrow cells were isolated and expanded (MIAMI cells). For transplantation studies, EGF-bFGF pre-treated cells were used as such in some cases or were further induced toward a dopaminergic phenotype (DI-MIAMI cells). Female Sprague Dawley rats, 12 weeks of age, ~250 g, received two injections stereotactically of 10 µg 6-hydroxydopamine (6-OHDA) in 5 µL saline supplemented with 0.1% ascorbic acid to induce a unilateral and partial progressive and retrograde lesion of the nigrostriatal system. Only rats that showed more than 7, but less than 18, net ipsiversive turns per minute at 11 days after the lesion were used. At 2 weeks post-lesion, 1.5×10^5 cells alone or attached to 0.75 mg PAMs were stereotactically injected into the lesioned striatum. Transplantation of DI-MIAMI cells adhered onto PAMs-NT3 strongly and significantly decreased amphetamine-induced rotational behavior compared to sham-treated rats or rats implanted with cells alone. The rotational behavior was linked to the integrity of the lesioned nigrostriatal pathway, as shown using a rat-specific anti-TH immunohistochemistry. Only a few TH-positive fibers remained in the striatum of sham-treated rats 8 weeks after the lesion, suggesting that the retrograde neurodegeneration progressed in time concomitantly with the increased rotational behavior. The number of neurons in the ipsilateral substantia nigra (SN) was also importantly decreased compared to the contralateral side. Transplantation of DI-MIAMI cells in combination with PAMs resulted in a significantly higher density of TH-positive fibers in the lesioned striatum, thereby demonstrating their neurorepair properties. However, a higher number of dopaminergic neurons were also observed in the ipsilateral SN in 40% of the animals, suggesting that a neuroprotection of the nigrostriatal pathway occurred in addition to a repair mechanism due to fiber outgrowth. Transplantation of DI-MIAMI cells without PAMs induced only a small, non-significant protection of the striatal dopaminergic fibers compared to sham-treated rats.

Functionalized composite scaffolds

Collagen-chitosan porous scaffolds with a volume size of 3.0 mm × 3.0 mm × 2.0 mm were produced by Yan et al. (2019). Bone marrow mesenchymal stem cells (BMSCs) were obtained from the bone marrow of all four limbs of male Wistar rats, 3 weeks of age, 100 g, and cultured using a complete bone marrow adherence method (Zhao et al., 2011). Passage 3 cells were purified, and at 48 hours prior to cell transplantation, 10 µM BrdU was added to the culture medium to label the BMSCs. Each scaffold was cultured with BrdU-labeled BMSCs at 2×10^6/µL to allow cell adherence within the scaffold. The porosity of the collagen-chitosan scaffold was 90%, and the scaffold gradually degraded within 1 month *in vitro* and *in vivo*, which provided the necessary microenvironment for BMSCs to grow and migrate. A TBI model using male Wistar rats, 12 weeks of age (n = 44) was prepared using a controlled cortical impact procedure in which a 300 g weight was dropped from a height of 1 m onto the exposed parietal bone. At 72 hours after TBI, a scaffold seeded with BMSCs was placed directly into the lesion cavity induced in the left hemisphere by TBI. The neurological function of rats was assessed before TBI (day 0) and on days 1, 7, 14, and 35 after TBI using modified neurological severity scores (Mahmood et al., 2011). There were no significant changes in modified neurological severity scores on days 1 and 7 for rats that had received BMSCs/scaffold compared to rats in which BMSCs had been stereotactically injected. Compared to the control group (sham-treated), the modified neurological severity scores of rats in the experimental groups were significantly decreased on day 14. Histology of brain tissues revealed more degenerative cells in the hippocampus, cortex, and striatum on the lesion side in the control group than in the experimental groups. There was significantly greater vascular endothelial growth factor staining at the ischemic transplantation area and its surroundings (hippocampal dentate gyrus and subventricular zone) in the rats that had received BMSCs/scaffold compared to rats in which BMSCs had been stereotactically injected. Immunohistochemical staining on day 32 after transplantation showed that the growth and differentiation of the BrdU-labeled BMSCs in the brain occurred at different times following transplantation. BrdU-positive BMSCs were numerous in the damaged area, and eventually also numerous in the periphery of the damaged area after transplantation. Some of the differentiated neuron-like cells had already migrated to a maximum distance of 2 mm along the periphery of the infarcted area and even into normal brain tissues. They appeared circular and increasing. Neuron-specific enolase and glial fibrillary acidic protein (GFAP) were not expressed in BrdU-labeled BMSCs in the cortex and striatum after a short period following transplantation. On day 7, a few GFAP-positive and no neuron-specific enolase-positive BrdU-labeled BMSCs were observed; on day 14, more GFAP-positive and a few neuron-specific enolase-positive BrdU-labeled BMSCs were seen.

Wang et al. (2016) prepared poly(L-lactic acid) (PLLA) scaffolds by electrospinning a 10% (w/v) polymer solution. Aligned PLLA scaffolds were sectioned into short fibers 2–10 mm length and aminolyzed in 0.5% (v/v) ethylenediamine in isopropanol. Poly-D-lysine and 4-azidoaniline were covalently bound and reacted with xyloglucan under UV light. For *in vivo* application, the xyloglucan was prepared at 4.5% wt in Hank's balanced salt solution and subsequently diluted with cells at a ratio of 2:1 (i.e., the final concentration of 3% w/v) at the time of implantation. For *in vivo* studies, adult female Swiss mice were used as graft recipients while tyrosine hydroxylase-green fluorescent protein (TH-GFP) mice were used to generate embryos as a source of donor tissue (embryonic day 12.5) for transplantation. The use of TH-GFP donor tissue enabled identification of graft (GFP^+) *versus* host (GFP^-) derived TH^+ dopamine neurons *in vivo*. To model Parkinson's disease, mice received partial lesions of the ventral midbrain (VM) dopaminergic (DA) neurons by unilateral injection of 6-OHDA 3.2 µg into the SNpc. At 3 weeks post lesioning, host animals received ectopic intrastriatal grafts of

a single cell VM suspension. The cell suspension (15×10^4 cells/μL) was diluted 1:2 in either Hank's balanced salt solution, xyloglucan (±GDNF), or xyloglucan + PLLA short fibers (± glial-derived neurotrophic factor, GDNF) to give a final concentration of 5×10^4 cells/μL. GDNF was delivered within the cell preparation (Cells + soluble GDNF, 1 mg/injection), blended into the xyloglucan at the time of delivery with cells (Cells + XYLO-bGDNF, 1 mg/injection), delivered by immobilization of short fibers (Cells + XYLO + SF-iGDNF), or a combination of blended and immobilized (Cells + XYLO-bGDNF + SF-iGDNF). The various cell suspensions were stereotactically injected (2 μL, i.e., 10×10^4 cells) into the denervated host striatum. At 10 weeks after transplantation, animals were euthanized and brains removed. At 10 weeks post-implantation, neither xyloglucan nor the presence of PLLA short fibers at the graft site induced elevated levels of reactive astrocytes ($GFAP^+$) or microglia ($CD11b^+$) compared to cell implants alone. TH immunohistochemistry confirmed pronounced depletion of the host DA neurons in lesioned mice. GFP staining verified viable grafts, confined to the striatum in most (91%) of the mice. Quantification of GFP^+ cells revealed that the presence of xyloglucan, but not PLLA short fibers, significantly increased graft volume. The inclusion of GDNF (sGDNF) within the donor cell preparation at the time of implantation significantly improved the number of GFP^+ cells compared to cells alone. Incorporation of GDNF within the gel (bGDNF) induced a 2-fold increase in GFP^+ cell survival; however, the presentation of GDNF on the short fibers only (iGDNF) within the gel did not increase cell survival. Enhanced and prolonged GDNF delivery through a combination of both blending within the xyloglucan gel and tethering onto short fibers (XYLO-bGDNF + SF-iGDNF) resulted in a 3.7-fold increase in GFP^+ cells, significantly greater than all other methods of GDNF presentation. The ability of scaffold-delivered GDNF to promote the integration of GFP^+ DA grafted neurons was examined. Only sustained GDNF delivery enhanced graft-derived striatal innervation. Blending GDNF into the xyloglucan gel (+XYLO-bGDNF) resulted in a 2.1-fold increase in striatal innervation compared to cells alone, whilst blended plus immobilization GDNF (XYLO-bGDNF + SF-iGDNF) increased innervation by 3.1-fold.

Self-assembling peptides as scaffolds

In a study by Rodriguez et al. (2018) N-fluorenylmethyloxycarbonyl (Fmoc)-DIKVAV hydrogels, containing the IKVAV motif from laminin, were prepared at 20 mg/mL with self-assembly occurring at pH 7.4. Donor tissue for transplantation was obtained from time-mated mice expressing green fluorescent protein (GFP) under the tyrosine hydroxylase promoter (TH-GFP). Embryos at E12.5 were collected, TH-GFP^+ embryos were selected, their brains removed, and the VM dissected to isolate primary VM tissue which was dissociated in 0.1% DNase and 0.05% trypsin. Adult Swiss mice received unilateral microinjections of 6-OHDA 3 μg into the VM. At 3 weeks post lesioning, mice received implants of cells alone, cells + Fmo-DIKVAV, or cells + Fmoc-DIKVAV + GDNF (n = 7/group). Cells were implanted ectopically into the striatum. Cells were mixed at 1:1 ratio with Hank's balanced salt solution or Fmo-DIKVAV (±GDNF at 1 ng/μL) prior to implantation into the striatum. 2 μL (10×10^4 cells) was injected. After 10 weeks, mice were euthanized. The incorporation of GDNF within the Fmoc-DIKVAV hydrogel and its subsequent sustained delivery resulted in ~2-fold increase in the number of GFP^+ cells surviving after 10 weeks compared with cells + DIKVAV-SAP alone. The volume of innervation, measured as GFP^+ fiber innervation within the host striatum, was reduced when cells were transplanted in the presence of Fmoc-DIKVAV alone with a corresponding increase in the cell density. When delivered with GDNF, however, the volume of innervation was comparable to cells transplanted alone, suggesting that the prolonged release of GDNF from the gel was sufficient to overcome the restrictive growth with the hydrogel alone. The presence of Fmoc-DIKVAV and/or GDNF did not impair neurite extension and innervation of grafted VM cells into the host tissue.

Francis et al. (2016) encapsulated iPSCs infected with lentiviruses (termed iPSC-RN cells) within RADA16-1 microspheres (average diameter 106.9 ± 5.1 μm). To induce neuronal induction, iPSC-RNs were cultured in a medium supplemented with 10 ng/mL each of BDNF, GDNF, and NT3 and 2 μg/mL doxycycline, to induce *NeuroD1* and *EGFP* gene expression (iN cells). NOD-SCID IL2Rγc null mice, 20-35 g, were anesthetized. On day 8 after initiating neuronal induction, dissociated GFP^+ iN cells (10×10^4 cells/5 μL) or RADA-encapsulated GFP^+ iN cells (5 μL) were injected stereotactically into the striatum. Bilateral injections were made. At 3 weeks after transplantation, mice were euthanized. The immunohistochemical assay revealed that encapsulation of iNs within SAPNS (self-assembling peptide nanofiber scaffold) microspheres significantly increased survival *in vivo*. By counting cells within three representative 60 μm brain slices from each mouse, the fractional retention of injected cells was > 100-fold higher for the SAPNS-encapsulated iN system than that of dissociated iNs. The viability of cells within this volume was significantly greater for RADA16-1 encapsulated iNs compared to iNs in suspension, indicating a much higher survival rate of encapsulated cells based on the initial numbers injected. GFAP-positive astrocytes were seen surrounding both iNs transplanted in suspension and RADA16-1 encapsulated iNs. The scaffold-encapsulated neurons integrated well *in vivo* within the injection site, and extended neurites several hundred microns long into the host brain tissue.

Using RADA16-1-based SAPs that incorporate the ubiquitin receptor binding site RGD (Arg-Gly-Asp) functional motif (RADA16-RGD) and also the laminin-derived motifs bone marrow homing peptide BMHP1 (RADA16-BMHP1) and BHMP2 (RADA16-BMHP2), together with pure RADA16-1, 3D scaffolds were self-assembled on cell culture inserts, polyethylene terephthalate (PET) track-etched membrane, 1.0 μm pore size, in 24-well plates by Cunha et al. (2011). Adult NSCs were extracted from the subventricular zone of male C57BL/6 mice, 8 weeks of age, and expanded in a basal cell culture medium. 24 μL of each SAP was gently mixed with 8 μL of culture medium containing 4×10^3 cells/μL, i.e., a total of 3.2×10^4 cells. The mixture was placed on the insert membrane, which in turn was placed in the well containing basal cell culture medium for the proliferation assay and the basal cell culture medium supplemented with 20 ng/mL leukemia inhibitory factor and 20 ng/mL BDNF for cell differentiation and allowed to self-assemble at 37°C. After 5 days in culture, the PicoGreen assay was used to quantify total DNA in the scaffold as a measure of cell proliferation. All three functionalized SAPs RADA16-BMHP2, RADA16-BMHP1, RADA16-RGD performed better than RAD16 in promoting the proliferation of mouse NSCs. All SAPs and also RADA16 presented increased cell proliferation rates when the SAP concentration was decreased, so that the highest proliferation rates were obtained when SAPs were used at 0.5% (w/v). However, cell proliferation within any of the SAPs was not as high as in the 2D control condition. To evaluate the capacity of NSC to generate differentiated progeny, NSCs were cultured on the SAP scaffolds for 5 days. NSCs were then collected and plated on Cultrex coated coverslips and allowed to differentiate for 7 days. Each SAP scaffold influenced NSCs differently. RADA16-RGD had the highest number of cells differentiated and was significantly different from RADA16 and RADA16-BMHP1.

Micro-tissue engineered neural networks

O'Grady et al. (2020) reconstituted gelatin methacrylate (GelMA) in triethanolamine (TEOA) buffer to create a 10% (w/v) solution and pH was adjusted to 8.0–8.5. Scrambled (Ac-AGVGDHIGC to make GelMA-Scram) or N-Cadherin mimic (Ac-HAVDIGGGC to make GelMA-Cad) peptides were added to the GelMA-TEOA buffer to form a 0.1% (w/v) solution. After dialysis against deionized water (6–8 kDa cutoff), the pH of the solution was adjusted to 7.35–7.45, lyophilized, and stored at –20°C. To assess the ability of hydrogels to support human neuron survival and outgrowth, human iPSCs were differentiated into highly pure populations of cortical glutaminergic neurons and cultured for 70–100 days before use. The neurons were dissociated into single-cell suspensions rather than the more commonly used aggregates so that the effects of hydrogel encapsulation on survival could be better assessed. Neurons were embedded into Matrigel, GelMA-Cad, GelMA-Scram, or GelMA. As a negative control for physical conjugation of peptides to the hydrogels, neurons were also embedded in GelMA with either soluble N-cadherin peptide or soluble scrambled peptide. Neurons embedded in GelMA and GelMA-Scram (both conjugated and soluble peptide), as well as Matrigel with the soluble peptide, died within 4 days. By contrast, neurons in conjugated GelMA-Cad and Matrigel exhibited a viability of 90.2 ± 1.3% and 86.3 ± 2.2% after 2 days, respectively. After 3 days, neurons in conjugated GelMA-Cad exhibited viability of 96.7 ± 1.2% while viability in Matrigel decreased slightly to 80 ± 1.3%. Neurite projections from single-cell suspensions of neurons embedded in either Matrigel or conjugated GelMA-Cad after 5 and 10 days were monitored using calcein. On day 5, relative to Matrigel, individual neurons embedded in conjugated GelMA-Cad exhibited significantly higher average neurite length (28.9 ± 21.6 μm *vs.* 14.1 ± 2.6 μm), whereas average neurite width was not significantly different between conjugated GelMA-Cad and Matrigel (4.0 ± 0.2 μm *vs*. 3.7 ± 0.2 μm). However, on day 10, relative to Matrigel, individual neurons in conjugated GelMA-Cad had significantly higher average neurite length (67.2 ± 3.2 μm *vs.* 35.3 ± 7.1 μm) and average neurite width (6.8 ± 0.2 μm *vs*. 3.9 ± 0.2 μm). The increased length and width of neurites in conjugated GelMA-Cad suggested that neurons were being conferred with improved functional properties. Neurons embedded in conjugated GelMA-Cad expressed both synaptophysin (a presynaptic terminal marker) and PSD-95 (a postsynaptic terminal marker) 21 days after embedding, and there was an average colocalization of 87.3 ± 1.3%, indicating the formation of active synapses. Neurons embedded in Matrigel had substantially lower expression of synaptophysin and PSD-95, with only 13.3 ± 3.3% colocalization of the presynaptic and postsynaptic markers, indicating a lower number of functional synapses. Synaptic tracing experiments were performed by transducing iPSC-derived neurons with an adeno-associated virus encoding EGFP under the control of human synapsin promoter (where synapsin is a presynaptic terminal marker). Wild-type neurons were mixed with hydrogel precursor, and prior to crosslinking the hydrogels, a small population of adeno-associated virus-transduced neurons (1:100 ratio of transduced to non-transduced neurons) was injected into the center. The spread of the EGFP signal could be monitored over time to demonstrate functional synaptic connections. Limited EGFP spread was observed after 7 days, which was consistent with neurite length and width still increasing at this early time point. However, after 21 days, EGFP had propagated to many neurons within the conjugated GelMA-Cad hydrogels, whereas little EGFP spread was seen in Matrigel.

Micro-tissue engineered neural networks (micro-TENNs) consisting of an agarose ECM hydrogel molded into a cylinder through which axons could grow were made by Struzyna et al. (2018). The agarose cylinders with an OD 398 μm and ID 160 μm were cut to 6–12 mm in length and sterilized under UV light. 5 μL of an appropriate ECM cocktail was added to each micro-column. Primary mesencephalic neurons were isolated from the VM of time-pregnant Sprague-Dawley rats (embryonic day 14). Dopaminergic neuron aggregates were created based on previously described protocols (Ungrin et al., 2008) and were inserted into the ends of the agarose micro-columns. Based upon the depth and placement of the aggregates within the micro-column, micro-TENNs could be created that exhibited either externalized or internalized cell body regions. Moreover, this technique produced long

projecting unidirectional axonal tracts, as shown by TH and β-tubulin III immunoreactivity. As assessed by the length of the longest neurite in each micro-TENN, the axons projecting from the aggregates grew ~10× longer than analogous axons extending within micro-columns seeded with dissociated neurons. The use of engineered neuronal aggregates and specific ECM components were critical factors in axonal extension. The mean neuronal aggregate length at 14 days *in vitro* was 1165 ± 212 μm; therefore, the total micro-TENN length (neuronal aggregate + axon length) attained using dopaminergic aggregates in collagen was > 6 mm by 14 days *in vitro* which was suitable to span the nigrostriatal pathway in rats. The capacity of the micro-TENNs to release dopamine *in vitro* was examined. At 24 days *in vitro*, a carbon fiber electrode was used to record evoked dopamine release in both the dopaminergic aggregate as well as at the distal end of the micro-column containing the terminals of the axonal tracts. Following incubation in media containing L-DOPA, dopamine release could be elicited in both the somatic and axonal regions. As the dopaminergic axons comprising the nigrostriatal pathway synapse with striatal neurons in the brain, the ability of the tissue-engineered nigrostriatal pathway to synapse with a population of striatal neurons *in vitro* was examined. Dopaminergic micro-TENNs were generated and after 10 days *in vitro*, embryonic rat striatal aggregates were inserted into the vacant ends of the micro-columns. After 4 more days *in vitro*, immunocytochemistry was performed to assess potential synaptic integration between the two populations. This confirmed the presence of the appropriate neuronal subtypes in the two aggregate populations, specifically TH^+ dopaminergic neurons and $DARPP\text{-}32^+$ medium spiny striatal neurons. Confocal microscopy revealed extensive axonal-dendritic integration and positive synapse formation involving the dopaminergic axons and striatal neurons. Also, immunocytochemistry confirmed that the majority of the striatal ($DARPP\text{-}32^+$) neurites were also $MAP\text{-}2^+$, suggesting that these were dendrites. Dopaminergic aggregate micro-TENNs with an inner lumen containing collagen 1 (in some instances transduced to express GFP) were grown for 14 days *in vitro*, after which time they were drawn into a custom needle and stereotactically microinjected to approximate the nigrostriatal pathway in adult male Sprague-Dawley rats. Animals were euthanized after 15 minutes, 1 week or 1 month (*n* = 5 each). The tissue of animals that were euthanized after 15 minutes was labeled with the dopaminergic marker TH to confirm that the transplantation process itself did not harm the micro-TENN cytoarchitecture, revealing surviving construct neurons in the substantia nigra and maintenance of their axonal projections within the micro-column towards the striatum. At 1 week and 1 month time points, surviving GFP^+ neurons and axons were found within the micro-TENN lumen, which were easily identified spanning the nigrostriatal pathway since the agarose micro-column had only partially degraded at these time points. Histological sections were co-labeled for the axonal marker β-tubulin III and the dopaminergic marker TH, revealing the preservation of a strong neuronal and dopaminergic axonal population. Longitudinally projecting TH^+ axons were present which confirmed that the micro-TENNs were mostly able to maintain their cytoarchitecture following longer-term transplantation into the brain. Micro-TENNs were also fabricated with aggregated dopaminergic neurons differentiated from human embryonic stem cells using a previously described protocol (Kriks et al., 2011). At 14 days following plating in the micro-columns, it was found that these micro-TENNs displayed the correct cytoarchitecture of a discrete somatic zone with unidirectional axonal tracts within the lumen of the hydrogel micro-column. These axonal extensions were > 4 mm in length at this time point.

Winter et al. (2016) fabricated micro-columns consisting of a thin molded cylinder composed of 3% agarose with a collagenous ECM on the interior to allow for astrocyte adhesion and growth. The hydrogel micro-columns had OD 798 μm–2 mm and ID 180 μm–1 mm, trimmed to 5 mm in most cases, and sterilized by UV light. 1–3 μL of a collagen ECM solution (0.5–2.0 mg/mL rat tail collagen type 1 in defined astrocyte medium) was microinjected into each. Extra-long micro-columns (10–30 mm) were also generated with OD 798 μm and ID 300 μm, with a proportionate amount of 1 mg/mL collagen microinjected. The micro-columns were placed in a humidified tissue culture incubator for 1 hour to allow the collagen to polymerize prior to the addition of cells. Primary cortical astrocytes were isolated from postnatal day 0–1 Sprague Dawley rat pups and dissociated. Over several weeks in culture, a nearly pure population of astrocytes (> 95%) was obtained. To seed astrocytes in the micro-columns, dissociated cell solution ($2–12 \times 10^5$ cells/mL) was microinjected into the micro-column. To ensure that the seeding density was held constant among micro-columns of different diameters, the astrocyte solution was made to the desired cell density and a sufficient volume was delivered to fill the entire internal canal of the cylinder; this entailed adding ~0.13 μL, 0.48 μL, 3.9 μL for 5 mm long micro-columns with 180 μm, 350 μm, and 1 mm IDs, respectively. Seeded micro-columns were placed in a humidified tissue culture incubator for 40 minutes to allow cells to adhere. Cerebral cortices were extracted from Sprague-Dawley rats (embryonic day 18) and dissociated to isolate cortical neurons. To assess the ability of the aligned astrocyte constructs to support neuron adhesion, survival, and neurite outgrowth, neurons were seeded by micropipetting 1–2 μL of neuron cell solution $2–4 \times 10^5$ cells/mL at the openings on both ends of micro-columns at 40 minutes following astrocyte seeding. These micro-columns were again placed in a humidified tissue culture incubator for 40 minutes to allow cells to adhere. Astrocytes grown in 1 mm ID micro-columns did not exhibit any preference in angle of process outgrowth, whereas astrocytes grown in 350 μm and 180 μm ID micro-columns demonstrated process alignment with the central axis of the hydrogel. 180 μm ID micro-columns produced the highest frequency of maximal alignment (i.e., processes that were 0° from the longitudinal axis). Astrocytes formed a continuously aligned network along the entire length of 5 mm hydrogel micro-columns, and immunocytochemistry confirmed that the construct was astrocytic throughout the entire length. Moreover, when constructed within longer micro-columns ranging from 2.0 to 3.0 cm in length, astrocytes formed a continuously aligned network of up to 2.5 cm. High-density micro-column seeding led to extensive astrocyte-collagen contraction along the length of the micro-column, resulting in continuous, dense 3D bundles of aligned bi-polar astrocytes measuring up to 150 μm in diameter yet extending to 2.5 cm. The structural integrity and stability of the longitudinally aligned astrocytic bundles were assessed by physically removing them from the hydrogel columns. The bundles of aligned bi-polar astrocytes were maintained despite gripping the end and applying tension for extraction, and once removed, without the structural support provided by the hydrogel scaffold. These bundles showed flexibility and maintenance of general alignment despite being physically manipulated. This demonstrated the durability and strength of the bundled astrocyte-collagen constructs and indicated their versatility for transplantation in or out of the hydrogel encasement. To assess the ability of the aligned astrocyte constructs to support neuronal survival and neurite outgrowth, neuronal-astrocytic cocultures within micro-columns were grown over several days *in vitro*. The co-seeded neurons survived and associated closely with bundles of longitudinally aligned astrocytes. Immunocytochemistry and confocal microscopy showed that at 4 days *in vitro*, neurons cocultured with astrocytes were attached to and extended neurites directly along the longitudinal bundles of aligned astrocytes. These growth patterns were in marked contrast to those observed on a 2D polystyrene surface, as neuronal adhesion and neurite outgrowth were only colocalized with astrocytes in some cases, and no preferential neurite growth alignment was seen. These findings demonstrate the ability of the aligned astrocyte micro-constructs to support neuron adhesion and survival as well as to provide structural and soluble cues to enable neurite extension directly along the aligned astrocyte somata and processes.

In an earlier study, Struzyna et al. (2015) manufactured micro-TENNs composed of an agarose ECM hydrogel molded into a cylinder through which axons could grow. The outer hydrogel structure consisted of 1–4% agarose and had OD 500–990 μm and ID 180–500 μm. The inner column was filled collagen (rat tail type I collagen 3.0 mg/mL), collagen-laminin (rat tail type I collagen 1.0 mg/mL; mouse laminin 1.0 mg/mL), or fibrin (salmon fibrin, 1.0 mg/mL fibrinogen with 0.5 U/mL thrombin). The micro-columns were incubated at 37°C for 30 minutes, cut to 4–35 mm length, and sterilized under UV light. Primary dorsal root ganglia (DRG) neurons (embryonic day 16) and cerebral cortical neurons (embryonic day 18) were obtained from Sprague-Dawley rats. DRG neurons were suspended at 5×10^6 cells/mL in the medium. Cerebral cortical neurons were suspended at 30×10^6 cells/mL in the medium. To create micro-TENNs, 5–10 μL of cell solution was delivered to one or both ends of the micro-columns. The micro-columns were placed in a humidified tissue culture incubator at 37°C for 50–75 minutes to allow cells to attach. Bidirectional micro-TENNs were created by seeding neuronal populations on both ends of the micro-columns, with the extension of neurites through the interior of the tube. This strategy encouraged DRG neuronal somata of the bidirectional constructs to form dense ganglia, predominantly restricted to the extremities. These ganglia projected long neurites into the interior, which, given sufficient time *in vitro*, overlapped and grew along each other. The neurites primarily extended along the border between the ECM internal core and the agarose walls of the micro-column. The length of neurite penetration in DRG neuron micro-TENNs was measured at weekly time points over 42 days *in vitro*. At 7 days *in vitro*, neurites extended 1.85 ± 0.62 mm into the micro-column interior. At 21 days *in vitro*, neurites penetrated 4.90 ± 1.25 mm, and by 42 days, axonal projections from bidirectional neurons had crossed the micro-column to form constructs measuring up to 2 cm. A collagen ECM alone in the micro-column interior did not adequately support cortical neuron survival and axon extension, resulting in almost complete neuronal death. However, both a salmon-derived fibrin matrix (1 mg/mL) and a laminin-collagen mixture (1 mg/mL LN and 1 mg/mL CoI) supported the health and outgrowth of primary cortical neurons within the micro-columns. The effects were assessed of micro-column agarose concentration (1–4%; affecting hydrogel stiffness and pore size) and dimensions (OD/ID combination; affecting wall thickness and thus diffusional distances) on neuronal viability and neurite outgrowth and health (with laminin-collagen as the inner core ECM). Neuronal viability did not vary across the range of agarose concentrations or OD/ID combinations that were evaluated. However, micro-TENNs fabricated with 3–4% agarose micro-columns maintained healthier neurites than those fabricated with 1–2% agarose. Neurite health did not vary across the various micro-column dimensions that were tested. Cortical neurons were induced to form dense 3D clusters consisting of discrete neuronal populations spanned by long fasciculated axonal tracts within the micro-columns. Based on the number of neurons seeded and the initial adhesion, both low-density and high-density cortical neuron micro-TENNs were generated. Immunocytochemistry and confocal microscopy revealed the presence of robust fasciculated and nonfasciculated axons ($\beta\text{-tubulin-III}^+$) that were observed projecting between neuronal clusters ($MAP\text{-}2^+$) as well as projecting along the length of the micro-column interior to form neuronal networks at various spatial scales. Immunocytochemical analysis demonstrated a negligible astrocytic population within the micro-TENNs (near absence of $GFAP^+$ cells/processes), which is consistent with the use of a defined (serum-free) culture media optimized for neuronal health but metabolically limiting for glial proliferation. A 4mm micro-TENN (7–10 days *in vitro* for either DRG neuron or cerebral cortical neuron micro-TENNs) was injected into the cortex of adult male Sprague-Dawley rats (*n* =

12). Histological examination and confocal microscopy revealed DRG neuron micro-TENNs survived within the micro-column at 3 days postimplantation (the only time point evaluated for DRG neuron micro-TENNs). The DRG neurons remained in a tight cluster with numerous axons projecting through the micro-column interior along the cortical-thalamic axis. Micro-TENNs generated using cerebral cortical neurons were also microinjected into naive rats along the cortical-thalamic axis. These pre-formed micro-TENNs consisted of GFP^+ cortical neurons to permit the identification of transplanted neurons/neurites *in vivo*. At both 7 and 28 days postimplantation, histological and confocal assessment demonstrated surviving GFP^+ micro-TENN neurons contained within the micro-column interior in both the cerebral cortex and the thalamus. These transplanted neurons exhibited a healthy morphology and maintained a neurite-bearing cytoarchitecture. Immunohistochemistry revealed that the GFP^+ longitudinal projections within the micro-TENNs consisted of aligned axons. Moreover, immunohistochemistry for the presynaptic protein synapsin revealed numerous synapses involving the neurons and neurites within the micro-TENNs, suggesting multiple synaptic relays along these projections. At the micro-column ends, histological examination showed that GFP^+ micro-TENN neurons extended numerous neurites into the host cortex. Interestingly, these neurites were predominantly projecting laterally from the micro-TENN extremity (at 90° to the cortical-thalamic axis). Neurites from micro-TENN neurons penetrated deep into the host cortex, generally of the order of 50–150 µm, but in some cases reaching lengths up to several hundred microns. Moreover, using confocal microscopy, putative dendritic spines along GFP^+ neurites projecting from the micro-TENNs were identified. Immunohistochemistry suggested that these neurites projecting from the micro-TENNs formed synapses with host neurons in the cerebral cortex.

The main findings regarding the ability of nano- and micro-sized constructs and scaffolds and hydrogels to promote neuronal survival and neurite outgrowth are summarized in **Tables 1** and **2**.

Discussion

Neurodegenerative diseases are increasing in prevalence in many countries and the medications currently approved by the FDA only bring about a temporary reduction of symptoms in patients with Alzheimer's or Parkinson's disease. Moreover, they do not slow or halt the progression of the disease, and often have undesirable side effects. Cell transplantation strategies offer an alternative approach to facilitating CNS repair, but efficacy is limited by low (1–2%) *in vivo* survival rates of cells that are injected in suspension (Tejeda et al., 2021). Transplanting cells that are attached to or encapsulated within a suitable biomaterial construct has the advantage of enhancing cell survival *in vivo*. Transplantation strategies using biomaterials required improvements in graft retention and were achieved by providing growth factors and neurotrophic factors (Bible et al., 2012). To restore functionality following major CNS injury requires promoting regeneration across the injury site, likely including both local neuronal cell replacement and reestablishment of long axonal tracts.

From the studies reviewed herein, a variety of biomaterials were used to make the constructs in different forms that included nanoparticles, nanotubes, microspheres, microscale fibrous scaffolds, and scaffolds as gels and micro-columns. Some of the studies had examined neuronal survival *in vitro* and/or *in vivo*, and included models of Alzheimer's disease, Parkinson's disease, and traumatic brain injury (**Tables 1** and **2**). Among the *in vitro* studies, Tween 80-treated mPEG-PLGA nanoparticles loaded with rhynchophylline had higher transport across a blood-brain barrier model and decreased cell death in a model of Alzheimer's disease than rhynchophylline or untreated nanoparticles with rhynchophylline (Xu et al., 2020). Using a model of Parkinson's disease, TAT bioconjugated with zwitterionic polymer poly(2-methacryoyloxyethyl phosphorylcholine) and protein-based nanoparticles loaded with non-Fe hemin had similar protective ability against MPTP-treated SH-SY5Y cells as free non-Fe hemin, and significantly decreased the level of reactive oxygen species in cells compared to untreated cells (Wang et al., 2017). Neuronal survival was examined in several studies using hydrogel encapsulated cells. Cortical glutaminergic neurons within gelatin methacrylate gel with N-cadherin mimic peptide exhibited high viability, high neurite length and width, and expressed both synaptophysin and PSD-95 (O'Grady et al., 2020). Using micro-columns consisting of an outer agarose gel cylinder and an inner lumen filled with ECM (collagen, fibrin, or laminin-collagen) and dopaminergic neuron aggregates produced from mesencephalic neurons isolated from the ventral midbrain of rats (embryonic day 14) inserted into the ends of the micro-columns, long projecting unidirectional axonal tracts were produced that were ~10× longer than analogous axons extending within micro-columns seeded with dissociated cells (Struzyna et al., 2018). In an earlier study using dorsal root ganglia neurons (embryonic day 16) and cerebral cortical neurons from rats (embryonic day 18) that were inserted at both ends of the micro-columns, long axonal tracts projecting through the interior of the micro-column were generated. A collagen ECM alone in the micro-column interior did not adequately support cortical neuron survival and axon extension, resulting in almost complete neuronal death. However, both a salmon-derived fibrin matrix and a laminin-collagen mixture supported the viability and outgrowth of cortical neurons within the micro-columns (Struzyna et al., 2015). Micro-columns consisting of an agarose cylinder with collagen ECM on the interior and seeded with dissociated astrocytes from rats (postnatal day 0–1) produced a continuously aligned astrocyte network along the entire length of the micro-column. Cerebral cortical neurons from rats (embryonic day 18) inserted at the openings of both ends of the micro-columns following astrocyte seeding became attached to and also then extended neurites directly along the longitudinal bundles of aligned astrocytes, showing that the aligned astrocyte constructs supported neuronal survival and neurite outgrowth (Winter et al., 2016).

Included among the *in vivo* studies were three studies on promoting neuronal survival and function. Microscale scaffolds created by electrospinning poly(desaminotyrosyl tyrosine ethyl ester carbonate) were downscaled and seeded with human neuronal induction (iN) cells and injected into the striatum of male NOD-SCID IL2 Ryc mice. At 3 weeks postinjection, there was a marked increase in survival of scaffold-seeded iN cells compared to injected dissociated cells (Carlson et al., 2015). In another study, iN cells

Table 1 | **Nano- and micro-sized biomaterial and tissue-engineered constructs to promote neuronal survival and neurite outgrowth in *in vitro* and *in vivo* studies**

Studies	Construct	Neurorestorative effects of constructs
Nanoparticles delivery and carbon nanotubes for cell engraftment		
Maraei et al., 2017	Multiwalled carbon nanotubes (MWCNT) OD ~50–60 nm, length ~10–20 µm mixed with human OBNSCs neurospheres	CNT/OBNSCs mixture injected at CA1 of the hippocampus in TMT-treated Wistar rats and after 8 wk morphological criteria suggestive of mature neurons were seen. Engrafted cells differentiated into neurons, oligodendrocytes, and astrocytes.
Wang et al., 2017	TAT-NFH-nBSA nanoparticles, size ~24 nm	TAT-NFH-nBSA nanoparticles had similar cell viability against MPTP-treated SH-SY5Y cells *in vitro* as free NFH and decreased the ROS level in cells compared to untreated cells. TAT-NFH-nBSA nanoparticles given i.v. to MPTP-treated C7BL/6 mice caused Parkinsonian symptoms to be reversed and included a greater increase in body weight and improvement in two behavioral tests. TAT-5-NFH-nBSA caused an increase in mRNA of TH and DAT.
Xu et al., 2020	T80-mPEG-PLGA nanoparticles (NPS)-RIN, mean size 145 nm	Higher transport across BBB *in vitro* model than RIN or NPS-RIN. Decreased PC12 cell death *in vitro* by $A\beta_{25-35}$ compared to RIN.
Microspheres and microscale scaffolds		
Delcroix et al., 2011	PAMs consisting of PLGA microspheres, 60 µm diameter, coated with laminin and PDL and release NT3 and used to attach human DI-MIAMI cells (generated from cells of a 3-yr-old male cadaver)	6-OHDA injected stereotactically into female Sprague-Dawley rats, 12 wk of age, to induce unilateral lesion of the nigrostriatal system. At 2 wk post-lesion, DI-MIAMI cells or attached to PAMs were injected into lesioned striatum. Transplantation of DI-MIAMI cells in combination with PAMs protected dopaminergic neurons in lesioned striatum, and also in ipsilateral substantia nigra in 40% of animals. Amphetamine-induced rotational behavior was significantly decreased by transplantation of DI-MIAMI with PAMs compared to sham rats or cells alone.
Carlson et al., 2015	Microscale scaffolds 100 µm square created from pDTEc fibrous microspun substrate fiber diameter 3.23 µm were downscaled to which human iN cells were seeded in suspension	Scaffold-supported or dissociated iN cells were injected into the striatum of male NOD-SCID IL2 Ryc null mice, 20–35 g. At 3 wk post-transplantation, there was a 38-fold improvement in an average survival rate of injected scaffold-seeded iN cells compared to injected dissociated iN cells. The scaffold-seeded cells maintained neurite length, comparable to that of viable dissociated cells.
Skop et al., 2019	Heparin crosslinked to chitosan microspheres ~50 µm diameter to which was attached VZ NPs from rat neocortex (embryonic d 13.5)	VZ NPs on microspheres injected into lesion cavity at 7 d after CCI in male Sprague Dawley rats, 2 mon of age; at 2 wk post-transplantation lesion cavity was smaller than in controls that received cells or microspheres only.

6-OHDA: 6-Hydroxydopamine; $A\beta_{25-35}$: amyloid β25–35; BBB: blood-brain barrier; CCI: controlled cortical impact; DAT: dopamine transporter; DI-MIAMI: dopaminergic marrow-isolated adult multilineage inducible cell; pDTEc: poly(desaminotyrosyl tyrosine ethyl ester carbonate); iN: induced neural cell; MPTP: 1-methyl-4-phenyl-1,2,3,6-tetrahydropyridine; NT3: neurotrophin 3; OBNSC: olfactory bulb neural stem cell; PAM: pharmacologically active microcarriers; PDL: poly-D lysine; RIN: rhynchophylline; ROS: reactive oxygen species; TAT-NFH-nBSA: HIV-1 trans-activating transcriptor- non-Fe hemin-bovine serum albumin; TH: tyrosine hydroxylase; T80-mPEG-PLGA: Tween 80-methoxy poly(ethylene glycol)-poly(lactic-co-glycolic acid);VZ: ventricular zone.

Table 2 | **Scaffold and hydrogel constructs to promote neuronal survival and neurite outgrowth in *in vitro* and *in vivo* studies**

Studies	Construct	Neurorestorative effects of constructs
Functionalized composite scaffolds		
Wang et al., 2016	PLLA scaffolds cut into short fibers 2–10 mm in length, aminolyzed, and PDL and 4-azido-aniline covalently bound and reacted with xyloglucan under UV light	6-OHDA injected into SNpc of female adult Swiss mice and at 3 wk after lesioning mice received an intrastriatal injection of single-cell suspension of VM from TH-GFP mice (embryonic day 12.5). The cell suspension was diluted in either medium, xyloglucan (± GDNF), or xyloglucan + PLLA short fibers (± GDNF). Inclusion of GDNF within donor cell preparation or the gel increased GFP^+ cell survival. Blending GDNF into xyloglucan gel or blended plus immobilization GDNF increased striatal innervation.
Yan et al., 2019	Collagen-chitosan scaffolds 3 mm × 3 mm × 2 mm with BMSCs from male Wistar rats at 3 wk of age	At 72 h after CCI in male Wistar rats, 12 wk of age, a scaffold seeded with BMSCs was placed in lesion cavity in the left hemisphere; on d 14, mNSS score was decreased compared to the sham group and $GFAP^+$ and a few NSE^+ BrdU-labeled BMSCs were seen in the cortex and striatum.
Self-assembling peptides (SAPs) as scaffolds		
Francis et al., 2016	iPSC-RN cells encapsulated within RADA16.1 microspheres average diameter 107 µm and neuronal induction (iN) cells encapsulated within RADA16.1 microspheres	On d 8 after initiating neuronal induction, dissociated GFP^+ iN cells or RADA16.1-encapsulated GFP^+ iN cells were injected bilaterally into the striatum of NOD-SCID IL2Ryc null mice, 20–35 g. At 3 wk after transplantation, encapsulation of iNs within SAPNS microspheres increased survival *in vivo* compared to iNs in suspension. Scaffold-encapsulated neurons extended neurites into the host brain tissue.
Rodriquez et al., 2018	Fmoc-DIKVAV hydrogels were prepared with self-assembly occurring at pH 7.4	6-OHDA injected unilaterally into VM of adult Swiss mice. At 3 wk post lesioning, primary VM cells isolated from embryos at E12.5 were mixed with Fmoc-DIKVAV ± GDNF and implanted ectopically into the striatum. Incorporation of GDNF within Fmoc-DIKVAV hydrogel resulted in ~2-fold increase in GFP^+ cell survival after 10 wk.
Micro-tissue engineered neural constructs		
Struzna et al., 2015	Micro-column composed of an agarose cylinder OD 500–900 µm, ID 180–500 µm, 4–35 mm length and inner column filled with an ECM. Primary DRG neurons (embryonic day 16) and cerebral cortical neurons (embryonic day 18) were obtained from Sprague-Dawley rats and the cell suspension was delivered to one or both ends of micro-columns.	DRG neuronal somata of bidirectional constructs formed dense ganglia, mostly restricted to the extremities. These ganglia projected long neurites into the interior and primarily extended between the ECM internal core and the agarose walls of the micro-columns. By 42 d *in vitro*, axonal projections from bidirectional neurons formed constructs measuring up to 2 cm. A collagen ECM alone in the micro-column interior did not adequately support cortical neuron survival and axon extension. A salmon-derived fibrin matrix and a laminin-collagen mixture supported the health and outgrowth of primary cortical neurons within the micro-columns. A 4 mm micro-TENN (7–10 d *in vitro* for either DRG neuron or cerebral cortical neuron micro-TENNs) was injected into the cortex of adult male Sprague-Dawley rats. DRG neuron micro-TENNs survived within the micro-column at 3 d post-implantation. The DRG neurons remained in a tight cluster with numerous axons projecting through the micro-column interior along the cortical-thalamic axis. Micro-TENNs generated with GFP^+ cerebral cortical neurons were also injected along the cortical-thalamic axis. At 7 and 28 d post-implantation, histological and confocal assessment showed surviving GFP^+ micro-TENNs neurons contained within the micro-column interior in both the cerebral cortex and thalamus. At the micro-column ends, GFP^+ micro-TENN neurons extended numerous neurites into the host cortex. These neurites projecting from the micro-TENNs formed synapses with host neurons in the cerebral cortex.
Winter et al., 2016	Hydrogel micro-column consisting of agarose cylinder with collagen type 1 ECM interior, OD 798 µm–2 mm, ID 180 µm–1 mm, 5 mm length. Primary cortical astrocytes from post-natal day 0–1 Sprague-Dawley rats were seeded into the micro-column. Cortical neurons isolated from cerebral cortices of Sprague-Dawley rats (embryonic day 18) were seeded at both ends of micro-columns at 40 min following astrocyte seeding.	The co-seeded cortical neurons survived and were associated closely with bundles of longitudinally aligned astrocytes. At 4 d *in vitro*, neurons cocultured with astrocytes were attached to, and extended neurites directly along the longitudinal bundles of aligned astrocytes.
Struzyna et al., 2018	Micro-column consisting of an agarose cylinder OD 398 µm, ID 160 µm, 6–12 mm length, with ECM cocktail added to inner lumen. Dopaminergic neuron aggregates were inserted into the ends of the agarose micro-columns.	Dopaminergic neuron aggregates were inserted into the ends of agarose micro-columns which *in vitro* produced long projecting unidirectional axonal tracts. The axons projecting from the aggregates grew ~10 × longer than analogous axons extending within micro-columns seeded with dissociated cells. The total micro-TENN length (neuronal aggregate + axon length) using dopaminergic aggregates in collagen was > 6 mm by 14 d *in vitro* which was suitable to span the nigrostriatal pathway in rats. Dopaminergic neuron aggregates were created from VM mesencephalic neurons of Sprague-Dawley rats (embryonic day 14) and inserted into micro-column with inner lumen containing collagen 1 (in some instances transduced to express GFP) and grown for 14 d *in vitro* after which time they were stereotactically injected to approximate the nigrostriatal pathway in adult male Sprague-Dawley rats. At 1 wk and 1 mon, surviving GFP^+ neurons and axons were present within micro-TENN lumen, and were identified spanning the nigrostriatal pathway. Labeling sections with β-tubulin III and TH revealed the preservation of a robust neuronal and axonal population.
O'Grady et al., 2020	Scrambled to make GelMA-Scram or N-Cadherin mimic to make GelMA-Cad hydrogels were prepared. Human iPSCs were differentiated into cortical glutaminergic neurons and single-cell suspensions were encapsulated into Matrigel, GelMA-Scram, GelMA-Cad, or GelMA.	Neurons embedded in GelMA-Cad and Matrigel exhibited high viability while those embedded in GelMA-Scram or GelMA died within 4 d. On day 10, relative to Matrigel, neurons had higher average neurite length and width. At 21 d, neurons embedded in GelMA-Cad expressed both synaptophysin and PSD-95.

6-OHDA: 6-Hydroxydopamine; BMSC: bone marrow stem cell; BrdU: bromodeoxyuridine; CCI: controlled cortical impact; DRG: dorsal root ganglia; ECM: extracellular matrix; Fmoc-DIKVAV: N-fluorenylmethyloxycarbonyl-DIKVA; GDNF: glial-derived neurotrophic factor; GelMA: gelatin methacrylate; GFAP: glial fibrillary acidic protein; GFP: green fluorescent protein; iPSC-RN: induced pluripotent stem cells infected with lentiviruses effected by retronectin; mNSS: modified neurological severity score; NSE: neuron-specific enolase; PDL: poly-D-lysine; PLLA: poly(L-lactic acid); SAPNS: self-assembling peptide nanofiber scaffold; SNpc: substantia nigra pars compacta; TENN: tissue-engineered neural networks; TH: tyrosine hydroxylase; VM: ventral midbrain.

were encapsulated within RADA16.1 microspheres and injected bilaterally into the striatum of NOD-SCID IL2 Ryc mice. At 3 weeks after transplantation, RADA16.1 encapsulated iN cells had increased survival compared to iN cells in suspension and extended neurites into host brain tissue (Francis et al., 2016). Dopaminergic aggregates created from ventral midbrain mesencephalic neurons of rats (embryonic day 14) were inserted into an agarose micro-column with the inner lumen containing collagen and injected to approximate the nigrostriatal pathway in adult male Sprague Dawley rats. At 1 month posttransplantation, surviving neurons and axons were present within the micro-column lumen and spanned the nigrostriatal pathway (Struzyna et al., 2018).

Among the other *in vivo* studies reviewed were five that had used models of Parkinson's disease and two that had created a traumatic brain injury. TAT bioconjugated with zwitterionic polymer poly(2-methacryoyloxyethyl phosphorylcholine) and protein-based nanoparticles loaded with non-Fe hemin injected intravenously in MPTP-treated C57BL/6 mice induced a reversal of Parkinsonian symptoms. At a molar ratio of 5 for TAT to BSA, the nanoparticles loaded with non-Fe hemin caused an increase in mRNA level of tyrosine hydroxylase and dopamine transporter in the substantia nigra (Wang et al., 2017). Carbon nanotubes with olfactory bulb neural stem cells were injected at CA1 of the hippocampus in trimethyltin chloride-treated adult male Wistar rats and received daily immunosuppressive treatment.

The CA1 neurons and oligodendrocytes had increased in number at 4 weeks posttransplantation, and by 8 weeks the normal structure of the CA1 was regained with the restoration of pyramidal cell layer thickness (Maraei et al., 2017). 6-OHDA was injected stereotactically in adult female Sprague-Dawley rats to induce a unilateral lesion of the nigrostriatal system and at 2 weeks post-lesion DI-MIAMI cells or attached to PLGA microspheres coated with laminin and poly-D-lysine and designed to release neurotrophin 3 were injected into the lesioned striatum. DI-MIAMI cells were marrow-isolated adult multilineage inducible cells obtained from a young male cadaveric donor and induced towards a dopaminergic phenotype. Transplantation of DI-MIAMI cells attached to the microspheres protected dopaminergic neurons in the lesioned striatum and also in the ipsilateral substantia nigra in many (40%) of the animals (Delcroix et al., 2011). Substantia nigra pars compacta of adult female Swiss mice was injected with 6-OHDA and at 3 weeks after lesioning mice received an intrastriatal injection of a single cell suspension of neurons isolated from the ventral midbrain of TH-GFP mice (embryonic day 12.5). The cell suspension was mixed with poly-(L-lactic acid) scaffolds cut into short fibers, aminolyzed, and poly-D-lysine and 4-azido-aniline covalently bound and reacted with xyloglucan with/without glial-derived neurotrophic factor. Cell survival and striatal innervation were increased by including glial-derived neurotrophic factor within the gel (Wang et al., 2016). In addition, 6-OHDA was injected unilaterally into the ventral midbrain of Swiss mice, and at 3 weeks post lesioning primary neurons from ventral midbrain of embryos (embryonic day 12.5) were mixed with Fmoc-DIKVAV hydrogel with/without glial-derived neurotrophic factor and implanted into the striatum. Incorporating glial-derived neurotrophic factor within the hydrogel resulted in ~2-fold increase in cell survival after 10 weeks (Rodriquez et al., 2018). In the other series of studies, neural progenitors from the ventricular zone of rat neocortex (embryonic day 13.5) attached to chitosan microspheres crosslinked with heparin were injected into the lesion cavity at 7 days after controlled cortical impact procedure in adult male Sprague-Dawley rats. At 2 weeks posttransplantation, the lesion cavity was smaller than in control animals that received cells or microspheres only (Skop et al., 2019). A collagen-chitosan scaffold seeded with bone marrow-derived mesenchymal stem cells from young male Wistar rats was placed in the lesion cavity created in the left hemisphere at 72 hours after controlled cortical impact in adult male Wistar rats. The modified neurological severity score was decreased compared to sham-treated rats. A few neuron-specific enolase-positive bone marrow-derived mesenchymal stem cells were identified in the cortex and striatum on day 14 after transplantation (Yan et al., 2019).

Clearly from the cell transplantation studies reviewed, the incorporation of neurons within or attached to a suitable polymeric scaffold increased cell survival rate, neurite outgrowth, and formation of elongated axonal bundles. Furthermore, the inclusion of glial-derived neurotrophic factor had a positive effect on cell survival. While there were five *in vivo* studies in which cells had been transplanted in Parkinson's disease models, there were no such studies in which Alzheimer's disease or Huntington's disease models had been used. Certain medications especially those derived from herbs and used in traditional Chinese medicine have been shown to alleviate dementia and neurodegenerative syndrome with fewer side effects than conventional drugs (Wu et al., 2011). They are promising candidates for delivery attached to nanoparticles for intravenous injection and treated to facilitate transport across the blood-brain barrier. Interestingly, delivery of neurotrophin using nanoparticle-based controlled release formulations has been suggested as a procedure for inducing neuroregeneration processes towards the repair of neuronal damage (Angelova and Angelov, 2017).

Many of the transplantation studies had utilized cells isolated from the brains of mouse or rat embryos; however, the use of cells from human embryos or fetuses (abortion) in clinical studies would raise possible ethical concerns. Obtaining neural stem cells from the adult human olfactory bulbs would allow transplantation for neurodegenerative diseases and traumatic brain injury, and thus provide biosafety, biocompatibility, and not raise the ethical issues connected with the use of embryonic or fetal material (Curtis et al., 2007). In previous studies, neural stem cells were isolated from the human olfactory bulb, proliferated in culture, and then engrafted in a rat model of Alzheimer's disease, Parkinson's disease, and spinal cord injury. These studies demonstrated the ability of engrafted human olfactory bulb neural stem cells to proliferate, differentiate into different neuronal and glial elements, and restore cognitive and motor deficits associated with Alzheimer's disease (Marei et al., 2015a) and Parkinson's disease (Marei et al., 2015b). The Alzheimer's disease model used rat hippocampus treated with ibotenic acid, a neurotoxicant specific to hippocampal cholinergic neurons that are lost in Alzheimer's disease (Marei et al., 2015a).

The first clinical transplantation trials using pluripotent stem cells as donor tissue for the treatment of Parkinson's disease patients began in Japan in 2018 (Viviescas, 2019). A single surgery could potentially provide a transplant that would last throughout a patient's lifespan, reducing or altogether avoiding the need for dopamine-based medications. At present, clinical trials of cell transplantation for Parkinson's disease are in progress using fetal ventral mesencephalic cells (Clinicaltials.gov, NCT01898390), embryonic stem cells (NCT02452723, NCT03119636), neural progenitor cells (NCT03309514), and induced pluripotent stem cells (Schweitzer et al., 2020; Takahashi, 2020), involving injection into the striatum and substantia or basal ganglia structures (for review see Jang et al., 2020). Clinical trials of cell transplantation in patients with Alzheimer's disease are also ongoing (ClinicalTrials.gov, NCT01547689, NCT02672306, NCT02054208, NCT02600130) and involve intravenous or intraventricular injection in patients (see Liu et al, 2020). However, it appears that none of these trials are utilizing tissue-engineered constructs to improve the viability of cells transplanted into the brains of patients.

In conclusion, cell transplantation strategies using biomaterial constructs or systemic administration of functionalized nanoparticles have the potential to become an effective treatment modality for patients with neurodegenerative disease or traumatic brain injury. Future studies are warranted in animal models of Parkinson's disease and Alzheimer's disease using various types of cells or substances obtained from Chinese herbs that could be of potential benefit in new clinical trials. The use of micro-columns to transplant cells in animal models of Parkinson's disease and Alzheimer's disease should also be examined. These studies should be performed with both male and female animals and include behavioral testing in the Parkinson's and Alzheimer's disease models. In addition, experiments will be necessary using non-human primates to test the efficacy and safety of the two strategic approaches to check there are little or no off-target effects with using functionalized nanoparticles and tumor formation does not occur with stem cell transplantation. Recently it has been shown that transplanting autologous induced pluripotent stem cells into the brain of Parkinsonian monkeys without immunosuppression brought about recovery from motor and depressive behaviors (Tao et al., 2021). It would be useful to study the additive effects of several experimental regimens and determine whether or not these unique approaches demonstrate therapeutic synergism.

Author contributions: *Both authors approved the final version of the manuscript.*
Conflicts of interest: *There are no conflicts of interest.*

References

Anderson AJ, Haus DL, Hooshmand MJ, Perez H, Sontag CJ, Cummings BJ (2011) Achieving stable human stem cell engraftment and survival in the CNS: is the future of regenerative medicine immunodeficient? Regen Med 6:367-406.
Angelova A, Angelov B (2017) Dual and multi-drug delivery nanoparticles towards neuronal survival and synaptic repair. Neural Regen Res 12:886-889.
Ayton S, Lei P, Duce JA, Wong BX, Sedjahtera A, Adlard PA, Bush AI, Finkelstein DI (2013) Ceruloplasmin dysfunction and therapeutic potential for Parkinson disease. Ann Neurol 73:554-559.
Bible E, Qutachi O, Chau DY, Alexander MR, Shakesheff KM, Modo M (2012) Neo-vascularization of the stroke cavity by implantation of human neural stem cells on VEGF-releasing PLGA microparticles. Biomaterials 33:7435-7446.
Borisoff JF, Chan CC, Hiebert GW, Oschipok L, Robertson GS, Zamboni R, Steeves JD, Tetzlaff W (2003) Suppression of Rho-kinase activity promotes axonal growth on inhibitory CNS substrates. Mol Cell Neurosci 22:405-416.
Bradbury EJ, Moon LD, Popat RJ, King VR, Bennett GS, Patel PN, Fawcett JW, McMahon SB (2002) Chondroitinase ABC promotes functional recovery after spinal cord injury. Nature 416: 636-640.
Cai J, Peng X, Nelson KD, Eberhart R, Smith GM (2005) Permeable guidance channels containing microfilament scaffolds enhance axon growth and maturation. J Biomed Mater Res Part A 75:374-386.
Carlson AL, Bennett NK, Francis NL, Halikere A, Clarke S, Moore JC, Hart RP, Paradiso K, Wernig M, Kohn J, Pang ZP, Moghe PV (2016) Generation and transplantation of reprogrammed human neurons in the brain using 3D microtopographic scaffolds. Nat Commun 7:10862.
Cheng HC, Ulane CM, Burke RE (2010) Clinical progression in Parkinson disease and the neurobiology of axons. Ann Neurol 67: 715-725.
Cordeiro KK, Cordeiro JG, Furlanetti LL, Garcia Salazar JA, Tenório SB, Winkler C, Döbrössy MD, Nikkhah G (2014) Subthalamic nucleus lesion improves cell survival and functional recovery following dopaminergic cell transplantation in parkinsonian rats. Eur J Neurosci 39:1474-1484.
Cullen DK, R Patel A, Doorish JF, Smith DH, Pfister BJ (2008) Developing a tissue-engineered neural-electrical relay using encapsulated neuronal constructs on conducting polymer fibers. J Neural Eng 5:374-384.
Cummings BJ, Uchida N, Tamaki SJ, Salazar DL, Hooshmand M, Summers R, Gage FH, Anderson AJ (2005) Human neural stem cells differentiate and promote locomotor recovery in spinal cord-injured mice. Proc Natl Acad Sci U S A 102:14069-14074.
Cunha C, Panseri S, Villa O, Silva D, Gelain F (2011) 3D culture of adult mouse neural stem cells within functionalized self-assembling peptide scaffolds. Int J Nanomedicine 6:943-955.
Curinga G, Smith GM (2008) Molecular/genetic manipulation of extrinsic axon guidance factors for CNS repair and regeneration. Exp Neurol 209:333-342.
Curtis MA, Kam M, Nannmark U, Anderson MF, Axell MZ, Wikkelso C, Holtås S, van Roon-Mom WM, Björk-Eriksson T, Nordborg C, Frisén J, Dragunow M, Faull RL, Eriksson PS (2007) Human neuroblasts migrate to the olfactory bulb via a lateral ventricular extension. Science 315:1243-1249.
Delcroix GJ, Garbayo E, Sindji L, Thomas O, Vanpouille-Box C, Schiller PC, Montero-Menei CN (2011) The therapeutic potential of human multipotent mesenchymal stromal cells combined with pharmacologically active microcarriers transplanted in hemi-parkinsonian rats. Biomaterials 32:1560-1573.
Dewan MC, Rattani A, Gupta S, Baticulon RE, Hung YC, Punchak M, Agrawal A, Adeleye AO, Shrime MG, Rubiano AM, Rosenfeld JV, Park KB (2018) Estimating the global incidence of traumatic brain injury. J Neurosurg 130:1-18.
Filous AR, Miller JH, Coulson-Thomas YM, Horn KP, Alilain WJ, Silver J (2010) Immature astrocytes promote CNS axonal regeneration when combined with chondroitinase ABC. Dev Neurobiol 70:826-841.
Francis NL, Bennett NK, Haklikere A, Pang ZP, Moghe PV (2016) Self-assembling peptide scaffolds for 3-D reprogramming and transplantation of human pluripotent stem cell-derived neurons. ACS Biomater Sci Eng 2:1030-1038.
Fu AK, Hung KW, Huang H, Gu S, Shen Y, Cheng EY, Ip FC, Huang X, Fu WY, Ip NY (2014) Blockade of EphA4 signaling ameliorates hippocampal synaptic dysfunctions in mouse models of Alzheimer's disease. Proc Natl Acad Sci U S A 111:9959-9964.

Gelain F, Bottai D, Vescovi A, Zhang S (2006) Designer self-assembling peptide nanofiber scaffolds for adult mouse neural stem cell 3-dimensional cultures. PLoS One 1:e119.
Holmes TC, de Lacalle S, Su X, Liu G, Rich A, Zhang S (2000) Extensive neurite outgrowth and active synapse formation on self-assembling peptide scaffolds. Proc Natl Acad Sci U S A 97:6728-6733.
Horner PJ, Gage FH (2000) Regenerating the damaged central nervous system. Nature 407:963-970.
Huebner EA, Strittmatter SM (2009) Axon regeneration in the peripheral and central nervous systems. Results Probl Cell Diff 48:339-351.
Ikeda K, Ebina J, Kawabe K, Iwasaki Y (2019) Dopamine transporter imaging in Parkinson disease: progressive changes and therapeutic modification after anti-parkinsonian medications. Intern Med 58:1665-1672.
Jain A, Brady-Kalnay SM, Bellamkonda RV (2004) Modulation of Rho GTPase activity alleviates chondroitin sulfate proteoglycan-dependent inhibition of neurite extension. J Neurosci Res 77:299-307.
Jang SE, Qiu L, Chan LL, Tan EK, Zeng L (2020) Current status of stem cell-derived therapies for Parkinson's disease: from cell assessment and imaging modalities to clinical trials. Front Neurosci. 2020 14:558532.
Kim YT, Haftel VK, Kumar S, Bellamkonda RV (2008) The role of aligned polymer fiber-based constructs in the bridging of long peripheral nerve gaps. Biomaterials 29:3117-3127.
Kim SU, de Vellis J (2009) Stem cell-based cell therapy in neurological diseases: a review. J Neurosci Res 87:2183-2200.
Kim HJ (2011) Stem cell potential in Parkinson's disease and molecular factors for the generation of dopamine neurons. Biochim Biophys Acta 1812:1-11.
Kriks S, Shim JW, Piao J, Ganat YM, Wakeman DR, Xie Z, Carrillo-Reid L, Auyeung G, Antonacci C, Buch A, Yang L, Beal MF, Surmeier DJ, Kordower JH, Tabar V, Studer L (2011) Dopamine neurons derived from human ES cells efficiently engraft in animal models of Parkinson's disease. Nature 480:547-551.
Lei P, Ayton S, Finkelstein DI, Spoerri L, Ciccotosto GD, Wright DK, Wong BX, Adlard PA, Cherny RA, Lam LQ, Roberts BR, Volitakis I, Egan GF, McLean CA, Cappai R, Duce JA, Bush AI (2012) Tau deficiency induces parkinsonism with dementia by impairing APP-mediated iron export. Nat Med 18:291-295.
Levin PS, Newman SA, Quigley HA, Miller NR (1983) A clinicopathologic study of optic neuropathies associated with intracranial mass lesions with quantification of remaining axons. Am J Opthalmol 95:295-306.
Li Q, Chau Y (2010) Neural differentiation directed by self-assembling peptide scaffolds presenting laminin-derived epitopes. J Biomed Mater Res A 94:688-699.
Lindsay MP, Norrving B, Sacco RL, Brainin M, Hacke W, Martins S, Pandian J, Feigin V (2019) World Stroke Organization (WSO): Global Stroke Fact Sheet 2019. Int J Stroke 14:806-817.
Liu K, Lu Y, Lee JK, Samara R, Willenberg R, Sears-Kraxberger I, Tedeschi A, Park KK, Jin D, Cai B, Xu B, Connolly L, Steward O, Zheng B, He Z (2010) PTEN deletion enhances the regenerative ability of adult corticospinal neurons. Nat Neurosci 13:1075-1081.
Liu XY, Yang LP, Zhao (2020) Stem cell therapy for Alzheimer's disease. World J Stem Cells 12:787-802.
Mahmood A, Qu C, Ning R, Wu H, Goussev A, Xiong Y, Irtenkauf S, Li Y, Chopp M (2011) Treatment of TBI with collagen scaffolds and human marrow stromal cells increases the expression of tissue plasminogen activator. J Neurotrauma 28:1199-1207.
Marchionini DM, Collier TJ, Camargo M, McGuire S, Pitzer M, Sortwell CE (2003) Interference with anoikis-induced cell death of dopamine neurons: implications for augmenting embryonic graft survival in a rat model of Parkinson's disease. J Comp Neurol 464:172-179.
Marei HE, Farag A, Althani A, Afifi N, Abd-Elmaksoud A, Lashen S, Rezk S, Pallini R, Casalbore P, Cenciarelli C (2015a) Human olfactory bulb neural stem cells expressing hNGF restore cognitive deficit in Alzheimer's disease rat model. J Cell Physiol 230:116-130.
Marei HE, Lashen S, Farag A, Althani A, Afifi N, A AE, Rezk S, Pallini R, Casalbore P, Cenciarelli C (2015b) Human olfactory bulb neural stem cells mitigate movement disorders in a rat model of Parkinson's disease. J Cell Physiol 230:1614-1629.
Marei HE, Elnegiry AA, Zaghloul A, Althani A, Afifi N, Abd-Elmaksoud A, Farag A, Lashen S, Rezk S, Shouman Z, Cenciarelli C, Hasan A (2017) Nanotubes impregnated human olfactory bulb neural stem cells promote neuronal differentiation in Trimethyltin-induced neurodegeneration rat model. J Cell Physiol 232:3586-3597.
Marshall VG, Bradley WG Jr, Marshall CE, Bhoopat T, Rhodes R (1988) Deep white matter infarction: correlation of MR imaging and histopathologic findings. Radiology 167:517-522.
Mingorance A, Solé M, Munetón V, Martínez A, Nieto-Sampedro M, Soriano E, del Río JA (2006) Regeneration of lesioned entorhino-hippocampal axons in vitro by combined degradation of inhibitory proteoglycans and blockade of Nogo-66/NgR signaling. FASEB J 20:491-493.
Moore MJ, Friedman JA, Lewellyn EB, Mantila SM, Krych AJ, Ameenuddin S, Knight AM, Lu L, Currier BL, Spinner RJ, Marsh RW, Windebank AJ, Yaszemski MJ (2006) Multiple-channel scaffolds to promote spinal cord axon regeneration. Biomaterials 27:419-429.
Nakaji-Hirabayashi T, Kato K, Iwata H (2013) In vivo study on the survival of neural stem cells transplanted into the rat brain with a collagen hydrogel that incorporates laminin-derived polypeptides. Bioconjugate Chem 24:1798-1804.
O'Grady BJ, Balotin KM, Bosworth AM, McClatchey PM, Weinstein RM, Gupta M, Poole KS, Bellan LM, Lippmann ES (2020) Development of an N-cadherin biofunctionalized hydrogel to support the formation of synaptically connected neural networks. ACS Biomater Sci Eng 6:5811-5822.
Orlacchio A, Bernardi G, Orlacchio A, Martino S (2010) Stem cells: an overview of the current status of therapies for central and peripheral nervous system diseases. Curr Med Chem 17:595-608.
Owen SC, Shoichet MS (2010) Design of three-dimensional biomimetic scaffolds. J Biomed Mater Res A 94:1321-1331.
Pang ZP, Yang N, Vierbuchen T, Ostermeier A, Fuentes DR, Yang TQ, Citri A, Sebastiano V, Marro S, Südhof TC, Wernig M (2011) Induction of human neuronal cells by defined transcription factors. Nature 476:220-223.
Peplow PV, Martinez B, Gennarelli TA (2021) Prevalence, needs, strategies, and risk factors for neurodegenerative diseases. In: Neurodegenerative Diseases Biomarkers, Towards Translating Research To Clinical Practice (Peplow PV, Martinez B, Gennarelli T, eds), pp3-8, New York:Springer Nature.
Rodriguez AL, Bruggeman KF, Wang Y, Wang TY, Williams RJ, Parish CL, Nisbet DR (2018) Using minimalist self-assembling peptides as hierarchical scaffolds to stabilise growth factors and promote stem cell integration in the injured brain. J Tissue Eng Regen Med 12:e1571-1579.
Schweitzer JS, Song B, Herrington TM, Park TY (2020) Personalized iPSC-derived dopamine progenitor cells for Parkinson's disease. N Eng J Med 382:1926-1932.
Semino CE, Kasahara J, Hayashi Y, Zhang S (2004) Entrapment of migrating hippocampal neural cells in three-dimensional peptide nanofiber scaffold. Tissue Eng 10:643-655.
Shao H, Mi Z, Ji WG, Zhang CH, Zhang T, Ren SC, Zhu ZR (2015) Rhynchophylline protects against the amyloid β-induced increase of spontaneous discharges in the hippocampal CA1 region of rats. Neurochem Res 40:2365-2373.
Shear DA, Tate MC, Archer DR, Hoffman SW, Hulce VD, Laplaca MC, Stein DG (2004) Neural progenitor cell transplants promote long-term functional recovery after traumatic brain injury. Brain Res 1026:11-22.
Silva GA, Czeisler C, Niece KL, Beniash E, Harrington DA, Kessler JA, Stupp SI (2004) Selective differentiation of neural progenitor cells by high-epitope density nanofibers. Science 303:1352-1355.
Silva NA, Salgado AJ, Sousa RA, Oliveira JT, Pedro AJ, Leite-Almeida H, Cerqueira R, Almeida A, Mastronardi F, Mano JF, Neves NM, Sousa N, Reis RL (2010) Development and characterization of a novel hybrid tissue engineering-based scaffold for spinal cord injury repair. Tissue Eng Part A 16: 45.
Skop NB, Singh S, Antikainen H, Saqcena C, Calderon F, Rothbard DE, Cho CH, Gandhi CD, Levison SW, Dobrowolski R (2019) Subacute transplantation of native and genetically engineered neural progenitors seeded on microsphere scaffolds promote repair and functional recovery after traumatic brain injury. ASN Neuro 11:1-21.
Stankowski JN, Dawson VL, Dawson TM (2012) Ironing out tau's role in parkinsonism. Nat Med 18:197-198.
Stichel CC, Hermanns S, Luhmann HJ, Lausberg F, Niermann H, D'Urso D, Servos G, Hartwig HG, Müller HW (1999) Inhibition of collagen IV deposition promotes regeneration of injured CNS axons. Eur J Neurosci 11:632-646.
Struzyna LA, Wolf JA, Mietus CJ, Adewole DO, Chen HI, Smith DH, Cullen DK (2015) Rebuilding brain circuitry with living micro-tissue engineered neural networks. Tissue Eng Part A 21:2744-2756.
Struzyna LA, Browne KD, Brodnik ZD, Burrell JC, Harris JP, Chen HI, Wolf JA, Panzer KV, Lim J, Duda JE, España RA, Cullen DK (2018) Tissue engineered nigrostriatal pathway for treatment of Parkinson's disease. J Tissue Eng Regen Med 12:1702-1716.
Takahashi J (2020) iPS cell-based therapy for Parkinson's disease: A Kyoto trial. Regen Ther 13:18-22.
Tallantyre EC, Bø L, Al-Rawashdeh O, Owens T, Polman CH, Lowe JS, Evangelou N (2010) Clinico-pathological evidence that axonal loss underlies disability in progressive multiple sclerosis. Mult Scler 16:406-411.
Tang XQ, Heron P, Mashburn C, Smith GM (2007) Targeting sensory axon regeneration in adult spinal cord. J Neurosci 27:6068-6078.
Tao Y, Vermilyea SC, Zammit M, Lu J, Olsen M, Metzger JM, Yao L, Chen Y, Phillips S, Holden JE, Bondarenko V, Block WF, Barnhart TE, Schultz-Darken N, Brunner K, Simmons H, Christian BT, Emborg ME, Zhang SC (2021) Autologous transplant therapy alleviates motor and depressive behaviors in parkinsonian monkeys. Nat Med 27:632-639.
Tate MC, Shear DA, Hoffman SW, Stein DG, Archer DR, LaPlaca MC (2002) Fibronectin promotes survival and migration of primary neural stem cells transplanted into the traumatically injured mouse brain. Cell Transplant 11:283-295.
Tate MC, García AJ, Keselowsky BG, Schumm MA, Archer DR, LaPlaca MC (2004) Specific beta1 integrins mediate adhesion, migration, and differentiation of neural progenitors derived from the embryonic striatum. Mol Cell Neurosci 27:22-31.
Tejeda G, Ciciriello AJ, Dumont CM (2021) Biomaterial strategies to bolster neural stem cell-mediated repair of the central nervous system. Cells Tissues Organs doi: 10.1159/000515351.
Theadom A, Mahon S, Hume P, Starkey N, Barker-Collo S, Jones K, Majdan M, Feigin VL (2020) Incidence of sports-related traumatic brain injury of all severities: a systematic review. Neuroepidemiology 54:192-199.
Trueman RC, Klein A, Lindgren HS, Lelos MJ, Dunnett SB (2013) Repair of the CNS using endogenous and transplanted neural stem cells. Curr Top Behav Neurosci 15:357-398.
Tsai EC, Dalton PD, Shoichet MS, Tator CH (2004) Synthetic hydrogel guidance channels facilitate regeneration of adult rat brainstem motor axons after complete spinal cord transection. J Neurotrauma 21:789-804.
Ungrin MD, Joshi C, Nica A, Bauwens C, Zandstra PW (2008) Reproducible, ultra high-throughput formation of multicellular organization from single cell suspension-derived human embryonic stem cell aggregates. PLoS One 3:e1565.
Vanni S, Baldeschi AC, Zattoni M, Legname G (2020) Brain aging: a lanus-faced player between health and neurodegeneration. J Neurosci Res 98:299-311.
Viviescas A (2019) Cell transplants could significantly improve Parkinson's treatment, study suggests. Parkinson's News Today. https://parkinsonsnewstoday.com/2019/02/21/stem-cell-transplant-improve-parkinsons-treatment/. Accessed August 8, 2021.
Wang TY, Bruggeman KF, Kauhausen JA, Rodriguez AL, Nisbet DR, Parish CL (2016) Functionalized composite scaffolds improve the engraftment of transplanted dopaminergic progenitors in a mouse model of Parkinson's disease. Biomaterials 74:88-98.
Wang N, Jin X, Guo D, Tong G, Zhu X (2017) Iron chelation nanoparticles with delayed saturation as an effective therapy for Parkinson disease. Biomacromolecules 18:461-474.
Wang R, Wang Z, Guo Y, Li H, Chen Z (2019) Design of a RADA16-based self-assembling peptide nanofiber scaffold for biomedical applications. J Biomater Sci Polym Ed 30:713-736.
Weinreb O, Mandel S, Youdim MBH, Amit T (2013) Targeting dysregulation of brain iron homeostasis in Parkinson's disease by iron chelators. Free Radical Biol Med 62:52-64.
Wen X, Tresco PA (2006a) Effect of filament diameter and extracellular matrix molecule precoating on neurite outgrowth and Schwann cell behavior on multifilament entubulation bridging device in vitro. J Biomed Mater Res Part A 76:626-637.
Wen X, Tresco PA (2006b) Fabrication and characterization of permeable degradable poly(DL-lactide-co-glycolide) (PLGA) hollow fiber phase inversion membranes for use as nerve tract guidance channels. Biomaterials 27:3800-3809.
Winter CC, Katiyar KS, Hernandez NS, Song YJ, Struzyna LA, Harris JP, Cullen DK (2016) Transplantable living scaffolds comprised of micro-tissue engineered aligned astrocyte networks to facilitate central nervous system regeneration. Acta Biomater 38:44-58.
Wu TY, Chen CP, Jinn TR (2011) Traditional Chinese medicines and Alzheimer's disease. Taiwan J Obstet Gynec 50:131-135.
Xu R, Wang J, Xu J, Song X, Huang H, Feng Y, Fu C (2020) Rhynchophylline loaded-mPEG-PLGA nanoparticles coated with Tween-80 for preliminary study in Alzheimer's disease. Int J Nanomedicine 15:1149-1160.
Yamauchi T, Kuroda Y, Morita T, Shichinohe H, Houkin K, Dezawa M, Kuroda S (2015) Therapeutic effects of human multilineage-differentiating stress enduring (MUSE) cell transplantation into infarct brain of mice. PLoS One 10:e0116009.
Yan F, Li M, Zhang HQ, Li GL, Hua Y, Shen Y, Ji XM, Wu CJ, An H, Ren M (2019) Collagen-chitosan scaffold impregnated with bone marrow mesenchymal stem cells for treatment of traumatic brain injury. Neural Regen Res 14:1780-1786.
Yip PK, Wong LF, Sears TA, Yáñez-Muñoz RJ, McMahon SB (2010) Cortical overexpression of neuronal calcium sensor-1 induces functional plasticity in spinal cord following unilateral pyramidal tract injury in rat. PLoS Biol 8:e1000399.
Zamproni LN, Mundim MTVV, Porcionatto MA (2021) Neurorepair and regeneration of the brain: a decade of bioscaffolds and engineered microtissue. Front Cell Dev Biol 9:649891.
Zhang S (2008) Designer self-assembling peptide nanofiber scaffolds for study of 3-D cell biology and beyond. Adv Cancer Res 99:335-362.
Zhang S, Gelain F, Zhao X (2005) Designer self-assembling peptide nanofiber scaffolds for 3D tissue cell cultures. Semin Cancer Biol 15:413-420.
Zhang Y, Pak C, Han Y, Ahlenius H, Zhang Z, Chanda S, Marro S, Patzke C, Acuna C, Covy J, Xu W, Yang N, Danko T, Chen L, Wernig M, Südhof TC (2013) Rapid single-step induction of functional neurons from human pluripotent stem cells. Neuron 78:785-798.
Zhao L, Feng ZH, Jiao SX, Li NN (2011) Culture condition and biological characteristics of rat bone marrow mesenchymal stem cells by using the whole bone marrow adherence method. Zhongguo Zuzhi Gongcheng Yanjiu yu Linchuang Kangfu 15:5923-5927.

C-Editors: Zhao M, Liu WJ, Qiu Y; T-Editor: Jia Y